UNIVERSITEIT VAN PRETORIA
UNIVERSITY OF PRETORIA
YUNIBESITHI YA PRETORIA

THE INLET EFFECTS OF MULTIPLE TUBES ON THE ADIABATIC PRESSURE DROP OF SMOOTH, HORIZONTAL TUBES, IN THE TRANSITIONAL FLOW REGIME

By

Erin Sarah Vause

Submitted in fulfilment of the requirements for the degree

MASTER OF ENGINEERING

In the Department of Mechanical and Aeronautical Engineering

University of Pretoria

December 2015

Supervisor: Prof J.P. Meyer

Abstract

There exists many investigations in the field of pressure drop inside smooth tubes; however, there is a research gap where this flow is in the transitional flow regime. All work in the transitional flow regime thus far has been concerned with a single tube and in limited cases the effect of different types of inlets were investigated. Many heat exchangers such as shell-and-tube heat exchangers consist of a number of closely packed tubes leading from a common header and in some cases may operate in or close to the transitional flow regime. However, it is not known what effect adjacent tubes will have on pressure drop and the flow distribution in the transitional flow regime. The purpose of this study is therefore to investigate the effect that the presence of adjacent tubes will have on the pressure drop in the transitional flow regime. The study is limited to smooth and circular, horizontal tubes in the fully developed, transitional flow regime and adiabatic pressure drops. The transition effects were investigated experimentally by developing and building an experimental set-up on which, firstly, the pressure drops could be measured of one tube to be used as a reference and then secondly, the pressure drop of three tubes in parallel, equally spaced, 1.4 diameters apart. The internal tube diameters of all tubes were 3.97 mm and the tube lengths were 6 m. The pressure drops were measured over a length of 1.97 m, at the end of the tubes where the flow was fully developed. The pressure drops were measured with pressure transducers while the inlet and outlet temperatures of the water were measured with PT100 probes. All the tubes were connected to a calming section to ensure a square-edge inlet. Experiments were conducted with water at Reynolds numbers from 700 to 5 100 to ensure that the pressure drops and thus friction factors could be determined for fully developed flow throughout the laminar, transitional and turbulent flow regimes. The uncertainty of the friction factors were all less than 1%. It was found that the centre tube experienced an earlier onset of transition than that previously seen in single tube tests, at a Reynolds number of 1 840. In the outer tubes, transitional flow was delayed well beyond that previously seen in literature. The flow in all three tubes underwent transition into fully developed turbulent flow by the maximum Reynolds number of 3 340. The effect of having multiple, adjacent inlets caused a maldistribution in the mass flow rate, with a 5.8% difference in the flow rates of the outer tubes in the transitional flow regime. New correlations were developed to predict the friction factor for transitional flow in each of three adjacent tubes at an inlet pitch distance of 1.4 times the inner tube diameter. Overall, it can be concluded that multiple tube entrances have an effect on the transitional flow in all of the tubes and should be further investigated for other pitch distance and tube arrangements.

Title:	The Inlet Effects of Multiple Tubes on the Adiabatic Pressure Drop of Smooth, Horizontal Tubes, In the Transitional Flow Regime
Supervisor:	Prof J.P. Meyer
Department:	Mechanical and Aeronautical Engineering
Degree:	Master in Engineering (Mechanical)

Acknowledgements

I would like to acknowledge the following people for their help and support:

- Professor J.P. Meyer
  For his role as supervisor and for sharing his expertise on the subject.

- Mr Danie Gouws
  For his help in the design and manufacture aspects of the project.

- Mr Andrew Hall and Mr Franscois Mulock Houwer
  For their assistance in the role of fellow researchers on this project.

- The institutions that provided support and funding:
  - University of Pretoria
  - National Research Foundation
  - The Department of Science and Technology
  - CSIR

Table of Contents

List of Figures

List of Tables

List of Symbols

English letters and symbols

A	Area
Cf	Skin friction coefficient
CSP	Concentrated Solar Power
D	Diameter
f	Darcy Weisbach friction factor
HVAC	Heating, Ventilation and Air-Conditioning
L	Length
$\dot{m}$	Mass flow rate
P	Pressure
Pr	Prandtl number
Re	Reynolds number
TEMA	Tubular Exchanger Manufacturers Association
V	Flow velocity

Greek symbols

ϵ	Surface roughness
Δ	Change
ρ	Density
μ	Dynamic viscosity

Subscripts

b	Bulk
c	Cross sectional
d	Diameter
FT	Fully turbulent
h	hydrodynamic
i	Inner
o	Outer
p	Pressure drop
s	Surface
t	thermal

1. Introduction

1.1. Background

An ever present challenge that faces humankind of the 21st century is the one of meeting the energy generation needs of a world with a fast growing population and continuous increase in industrialisation [1]. Heat exchangers form an essential part of the energy generation industry. The term 'heat exchanger' is self-defining: it is the term given to systems that function to exchange thermal energy. This exchange of heat is usually made between two fluids that are separated by a heat transfer surface. The use of heat exchangers is common and the industries in which they can be found are widely varied.

On a fossil fuel power plant heat exchangers form the boiler, which typically evaporates water using the heat of the combustion gases that are formed when the coal is burned. The steam that is generated is then used to drive steam turbines that in turn produce the electricity. However heat exchangers are an integral component of other power generation processes, such as solar and nuclear plants [2]. On CSP plants the Sun's energy heats up the surface of tubes that contain the working fluid. The hot fluid then passes through a heat exchanger where the thermal energy is transferred to water. The evaporated steam is used to drive a steam turbine that produces electricity [3]. In a nuclear energy system steam is similarly used to produce electricity. The thermal energy used to heat the working fluid is produced in the nuclear reactors. Specially designed heat exchangers transfer the thermal energy between the reactor plant and the steam generator plant.

Not only do heat exchangers form an integral part of the electricity generation system but they are also useful to human health in the waste water management systems. Waste water is pumped through large heat exchangers that keep the water at an ideal temperature that promotes the growth of bacteria-destroying microbes. Another industry in which heat exchangers make human life more comfortable is the HVAC industry. Buildings, refrigerators and motor vehicles are climate controlled by heat exchangers that can cool down or heat up the space by transferring thermal energy to the ambient air. In vehicles, heat exchangers also form the radiator, which is necessary to keep the internal combustion engine from overheating. Radiators on much smaller scale are used as heat sinks to keep electronic equipment from overheating.

Heat exchangers are used as refiners, reboilers and distillers on chemical plants; for example in the petroleum refining process. In the aerospace industry heat exchangers form part of the rocket engine cycle. The pumps and condensers receive energy from heat exchangers that remove unwanted heat from other parts of the system.

It is therefore clear that heat exchangers form an important part of many processes in today's technological age. The most common type of heat exchanger is the shell-and-tube design [4]. It is popular because of the versatility of its design and its ability to withstand harsh operating conditions. The design and manufacture of heat exchangers is very costly and it is greatly beneficial that efforts be made to make them as efficient as possible. In most of the energy generation methods mentioned above shell-and-tube heat exchangers are used.

Fluid flowing in tubes conforms to one of three different flow regimes: laminar, turbulent or transitional. With laminar flow the heat transfer through the tubes is small, because of the lack of mixing in the flow but there is a low pressure drop over the tube length. In the turbulent flow regime the heat transfer coefficient increases, as does the efficiency of the exchanger, but the pressure drop also increases and a higher pumping power is needed to drive the flow. For this reason the flow in heat exchanger tubes often falls in or close to the transitional flow regime in order to find a middle ground between the pressure drop and the heat transfer efficiency [2]. However, very little data exists regarding the transitional flow regime and its mechanisms. It is known to fluctuate and become unsteady so it is often avoided.

1.2. State of the Art in the Transitional Flow Regime

The state of the art work in the transitional flow regime will be presented here in three parts. First is a summary of the review conducted in the transitional flow regime that was delivered as a keynote address by Meyer at the 15th International Heat Transfer Conference [2]. Second is a review of the work that was completed and published after this conference. Third, is a discussion on all previous work that has considered the inlet effects of multiple tubes. This work is related to this study geometrical point of view, although no work was conducted in the transitional flow regime.

1.2.1. Summary of Previous Reviews

There is a lack of knowledge about the transitional flow regime: its exact flow mechanism is not fully understood, its benefit of heat transfer over pressure drop has not fully been quantified and the exact range in which it occurs is also unknown. Transition is expected to occur in the range of Reynolds number from 2 300 to 10 000. The start of the transition depends on *Re* and the effect of outside disturbances. Ghajar and his colleagues studied the effect that the tube inlet geometry has on the start of the transitional flow regime [5] [6] [7] [8]. Their research encompassed flow from all three flow regimes: laminar, transitional and turbulent and they measured the pressure drop and the heat transfer. They were able to develop friction factor and Nusselt number relations from their experimental data. They found that the smooth inlet of the bell-mouth delays transition and it occurs in the range from 5 100 to 6 100 Reynolds number. The re-entrant inlet geometry causes a much larger disturbance in the flow and transition occurs sooner: 2 900 <Re< 3 500. Heat transfer results published by Ghajar and Tam showed that the Reynolds number range in which transition occurs is a function of the distance from the inlet of the tube and the diameter of the tube. This variation from the inlet to the outlet can be explained by the variation in the viscosity of the fluid from the inlet to the outlet.

Ghajar and his colleagues ran their experiments by heating the tubes at a constant heat flux. They also concentrated their data measurements on the fully developed section of flow. Meyer and his colleagues also investigated transitional flow in smooth tubes [9] [10]. Their work differed from Ghajar's in several key aspects: they tested cooling instead of the heating of the tubes and they ran experiments using a constant wall temperature. They also introduced the hydrodynamically fully developed inlet shape. Their results corresponded with Ghajar's work.

Meyer and Olivier [11] [12] conducted similar investigations in the transitional flow regime using helically finned, enhanced tubes. Nunner [13] initially experimented with augmented tubes. He found that in the laminar region of flow the heat transfer was only marginally improved by the tube enhancement. Meyer found that the fins introduced a secondary transition that was caused by the fluid rotation introduced into the flow by the fins. Meyer discovered that in the laminar region the fins had a negative effect on the heat transfer because they interrupted the effects of secondary flow.

Meyer *et al.* [14] investigated the effect that nanofluids have on transition in the flow inside tubes. They tested aqueous solutions of carbon-walled nanotubes at a concentration of 0-1% inside smooth tubes. The presence of nanotubes disturbed the thermal and hydrodynamic boundary layer. This lead to an increased thermal conductivity of the base fluid and thus an enhanced Nusselt number. The disturbance caused transition to occur at lower Reynolds numbers and an increase in the nanotube concentration exacerbated this effect.

Further research at the University of Pretoria was conducted by Meyer into hysteresis effects [9]. Pressure drop and heat transfer measurements were taken, while slowly increasing the Reynolds number from the laminar region to the turbulent one. This process was then repeated in reverse. Plots and comparisons were drawn up to investigate the fluctuations in pressure drop and heat transfer between the two sets of results. According to Meyer and Olivier, the effects of hysteresis are negligible in the transitional flow regime.

It was suggested by Meyer in his address [2] that the following topics be given further consideration so as to develop the knowledge base of transitional flow:

a) The inlet effects of the calming section. The calming section was initially used by Ghajar to directionalise flow, however there exists no data to understand the inlet effects it causes and whether the design can be improved.
b) Upstream effects such as pulses and vibrations.
c) Different re-entrant geometry inlet lengths.
d) Tube bundles and the inlet effect that adjacent tubes have on one another, as well as the effect their spacing and layout have.
e) The effect that the attachment methods used to form tube bundles in industry have on the flow and heat transfer in the tubes.
f) Tube length and outlet effects, such as outlet shape curves in the tubes.
g) More thorough experiments using a constant wall temperature.
h) Annular passage tube flow and rectangular ducts.

1.2.2. More Recent Literature

In 2014, new research was published by Dirker *et al.* [15] that investigated similar transitional flow effects for rectangular micro-channels. Three different inlet geometries were studied: the sudden contraction, bell mouth and swirl inlet. The effect of these inlets on transition were studied for three different hydraulic diameters, namely 0.57, 0.85 and 1.05 mm. Adiabatic friction factors, as well as pressure drop and heat transfer at heat fluxes of 24, 36 and 48 kW/m^2 were investigated.

The results for the sudden contraction inlet corresponded well with previously generated correlations for rectangular channels in the laminar flow regime. For the adiabatic tests the critical Reynolds number was found to be between 1 800 and 2 000, while for the diabatic tests it was at 2 000. The other two inlets were tested mostly for the diabatic condition. In the laminar regime the friction factors were similar, however, in transition, they were higher than the friction factors exhibited by the sudden contraction inlet. It was found that the channel diameter to channel length ratio did not influence the critical Reynolds number.

Also in 2014, Everts [16] conducted research for a Master of Engineering thesis on the heat transfer and pressure drop in the transitional flow regime, focusing on the dynamics of the developing regime. She used water as the working fluid and build a test bench consisting of a 2.03 m long copper tube with an inner diameter of 11.52 mm. Both adiabatic and diabatic tests were run at Reynolds numbers between 500 and 10 000. Five flow regimes were defined so as to better understand and describe the developing flow characteristic. The laminar region yielded results similar to those found in literature. The developing laminar region differed from the laminar results found in fully developed flow. These effects also diminished along the length of the tube. The transitional flow regime was delayed in its onset and completion. It also occurred over a smaller band of Reynolds numbers than previously found for fully developed flow. Secondary flow effects were found to play a role, causing the diabatic friction factors to increase in the laminar flow region. Diabatic tests were run at heat fluxes of 6.5, 8 and 9.5 kW/m^2. In the turbulent regime the heat flux had negligible effect on the friction factors.

1.2.3. Related Literature

Work has been conducted by Wang *et al.* [17] to optimise a porous baffle with the aim of improving the flow distribution inside a heat exchanger. They used a numerical method to space the tube holes within the baffle and were able to improve the distribution of flow inside the tubes. Their experiments were conducted in the turbulent flow regime. Unfortunately this is some of the only research that attempts to understand the effect of multiple tubes on the flow distribution, but the effect on the heat transfer is still unquantified.

1.3. Problem Statement

Literature shows that all transitional flow research has been conducted for a single tube with different types of inlets. The types of inlets that were considered previously were square-edged, re-entrant, bell mouthed, and fully developed as shown schematically in Figure 1(a). However, this does not accurately mimic the actual inlet of tubes in a shell-and-tube heat exchanger (shown schematically in Figure 1(b) that operates in or close to the transitional flow regime.

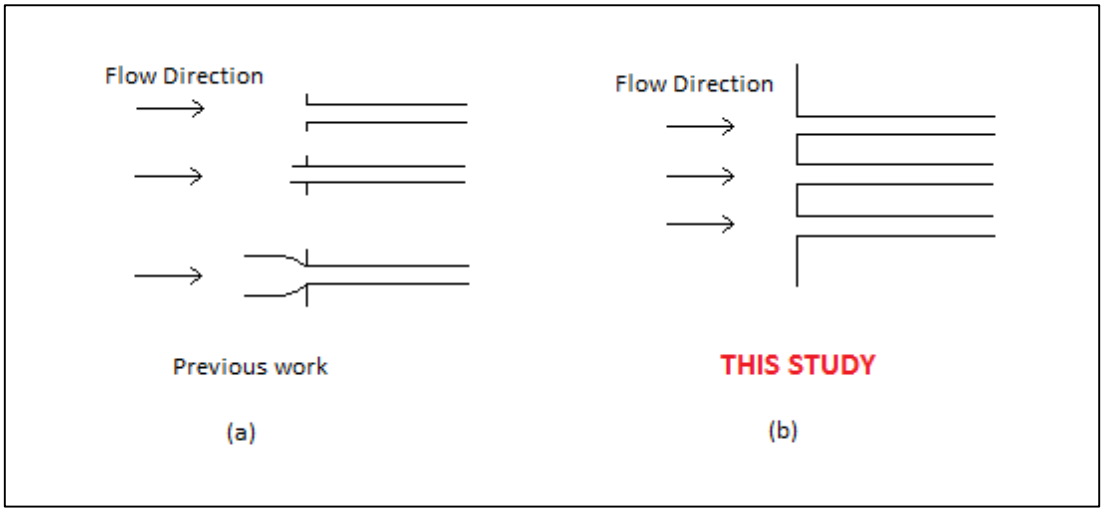

Figure 1.1: (a) Schematic of the different types of inlets used in previous studies of transitional flow in tubes. All inlets are for a single tube only. (b) Schematic of the inlet used in this study, with three adjacent tube inlets, all in a single plane.

In reality a multiple of tube bundles originate from a common header. As it has been shown from literature discussed in Section 1.2, that the shape of the inlet has an effect on transitional flow, it is reasonable to assume that the presence of neighbouring tubes may cause a disturbance that will alter the flow distribution. The pitch distance at which the tubes are spaced has not been investigated. The minimum pitch distance is specified by TEMA [18] to be 1.25 multiplied by the outer diameter of the tube. However, this value is based on the need for space to clean the fouling that builds up between the tubes. The closer the tubes are packed, the more tubes can be fitted inside a given shell space. Theoretically this means that there is a larger heat transfer surface area.

1.4. Justification

Shell-and-tube heat exchangers do not normally operate in the transitional flow regime but were designed to operate in the turbulent flow regime. However, Meyer [2] pointed out that more heat exchangers now operate in or close to the transitional flow regime for the following reasons:

a) When designing heat exchangers the cost of materials and manufacturing, safety, maintenance plans and risk of leakage must be taken into consideration. The transitional flow regime offers higher heat transfer than laminar flow but lower pressure drops than experienced in turbulent flow. Thus designing and building for these lower pressure conditions will be cheaper and operational conditions will be safer.
b) A heat exchanger may start to corrode and collect deposits with continued use. These deposits build up over time in the tubes and result in pressure drop changes, often bringing the mass flow rate into the transitional flow regime.
c) Manufacturers of shell-and-tube heat exchangers have the challenge that in regions of the world with very low winter temperatures, the water as working fluid has to be replaced with glycol mixtures with Prandtl numbers in the range of 30 to 100. At these high Prandtl numbers the fluid viscosities are very high and the pressure drops are so high that the mass flow rates have to be lowered, and the resulting flow conditions are close or in the transitional flow regime.

Furthermore, the maldistribution of the flow in heat exchangers must be considered since the operating conditions of the heat exchanger can induce maldistribution. This maldistribution can be viscosity induced, if the heat transfer across the tubes is not even or if fluid mixtures ae being used, such as the aforementioned glycol mixtures [4].

As literature showed, in the transitional flow regime the type of inlet has a significant effect on the flow characteristics. Therefore, it is reasonable to assume that a bank of tubes feeding into a header has a different type of inlet effect that has not yet been investigated. This type of inlet will directly influence the pressure drops and thus friction coefficients as already shown in literature (Section 1.2). The pressure drops are important as this affects pump energy usage that directly influence the operating costs of heat exchangers. It is therefore important to determine if pressure drop inlet effects occurs and if so, to quantify these effects. These results can be used by engineers to design more efficient heat exchangers in the transitional flow regime.

1.5. Aim of Study

The purpose of this study was to investigate the effect that the presence of multiple tube entrances have on the adiabatic pressure drop in smooth and circular, horizontal tubes in the fully developed, transitional flow regime.

1.6. Objective

The objectives of the study were as follows:

a) To design and build an experimental test setup that incorporates three smooth, horizontal tubes. The test section should be built so that three different tubes can be tested. Adiabatic pressure drop measurements must be taken in the transitional flow regime on this test bench. In order to capture the full transitional regime data from laminar and turbulent flow must also be present.
b) To quantify all of the inaccuracies of the test bench and its instrumentation devices.
c) To validate the pressure drop resulting data by testing a single tube on the bench and comparing it to previous studies.
d) To perform experiments on the test bench in the full developed transition flow regime, taking pressure drop measurements for three different tube pitch spacing.
e) To present the experimental results in a concise format.
f) To describe the results mathematically by formulating equations.

1.7. Scope of Work

This study is the outcome of a research masters that needed to be completed in nine months, with report writing and examination during month 10 to 12. A big part of this project was that the experimental set-up needed was designed and built from scratch. Limited technical assistance was available and with the work completed by myself and two other students (Franscois Mulock Houwer and Andrew Hall). Most of the time of this study was thus spend on building and commissioning the experimental set-up. There was thus very limited time to conduct experiments and the total time that was spend on experiments and report writing was about two months.

Because of time and cost the experimental set-up was limited to only one tube pitch spacing and to a testing arrangement with a maximum of three tubes, As this is a one-year long research Masters the experimental work conducted is limited to three round tubes in a simple horizontal, in-line arrangement. The addition of each extra tube requires an associated mass flow meter and this would increase the required cost significantly.

1.8. Outcomes

The outcomes of this investigation were to achieve fully developed transitional flow in two types of flow arrangements and to measure the pressure drops and to determine the friction factors. In the first flow arrangement, one tube was used as a reference tube. In the second arrangement three tubes were used. The results of the two arrangements were compared.

The original contribution that was made by this study was the comparison of the friction factor results of the configuration with three tubes to the configuration with a single tube as a function of Reynolds number. The Reynolds number range covered the laminar, transition, and turbulent flow regimes.

1.9. Overview of Dissertation

The dissertation will be divided into the following chapters, covering the below-mentioned material:

a) Chapter 2 presents a study on all the literature necessary to understand this topic, covering basic fundamentals, as well as previous research on the topic.
b) Chapter 3 contains a details description of the experimental test bench design as well as the operation procedure of the experimentation.
c) Chapter 4 presents the data of the validation tests as a proof of the validity of the study and results. This work is compared to previous research under the same conditions.
d) Chapter 5 contains the pressure drop results of the experiment, using three tubes.
e) Chapter 6 presents the summaries and conclusions of the study.

2. Literature Review

2.1. Introduction

The aim of this chapter is to summarise the fundamental concepts that are necessary to understanding adiabatic pressure drop and transitional flow, as well as to discuss relevant, previous studies in these fields. Firstly, the basic terminology is defined for use throughout the report. The theoretical equations defining adiabatic friction factor are analysed for use in validation of the results of this study. Finally, several previous studies are discussed and analysed, with the purpose to better understand pressure drop in the transitional flow regime for: smooth tubes, smooth tubes with various inlet shapes, microtubes and for nanofuids and developing flow. The chapter is concluded with a short summary and recommendations.

2.2. Fluid Flow and Heat Transfer: Basic Terminology

Reynolds Number

The regions in which laminar and turbulent flow occur are defined by the Reynolds number. Reynolds is a dimensionless number that describes the viscous behaviour of Newtonian fluids and was first described by Osborne Reynolds [19]. For flow in round ducts the Equation 2.2.1 can be used to calculate Reynolds number.

$$Re = \frac{\rho V D}{\mu} \tag{2.2.1}$$

For flow in smooth tubes, laminar flow occurs, approximately, for Reynolds numbers less than 2 300 and turbulent flow occurs in the range above 10 000. These can also be seen as the bounding values for the range in which transitional flow will occur. For this reason 2 300 is referred to as the critical Reynolds for internal flow in smooth round ducts. Transitional flow occurs between the critical *Re* and 10 000 but it is uncertain as to exactly where in this range the transitional flow will begin [20].

Friction Factor

The Darcy friction factor is a dimensionless parameter that is used to describe the friction losses in tube and channel fluid flow [20]. At low Reynolds numbers (laminar flow) this factor is dependent only on the Reynolds number and is independent of the surface roughness of a channel [21]. It can be computed, for circular tubes, using the Poiseuille [22] equation:

$$f = \frac{64}{Re} \tag{2.2.2}$$

The Darcy-Weisbach Equation (Equation 2.2.3) relates the pressure drop of fluid flow in a tube to the friction factor, as a function of mass flow ate, density and tube geometry. The friction factor and the pressure drop can be seen as directly proportional [20].

$$f = \frac{2\Delta P D}{L_p \rho V^2} \tag{2.2.3}$$

In previous literature the skin friction factor, *Cf*, is also sometimes used. This is equivalent to one quarter of the Darcy friction factor. The friction factor is further described by the Moody chart, discussed in Section 2.3.1.

2.3. Forced Internal flow

2.3.1. Moody Chart

The Moody chart was developed by Lewis Moody in 1944. It represents the Darcy friction factor as a function of Reynolds number and surface roughness for both laminar and turbulent flow in circular ducts.

The Moody chart describes the laminar region as a linear relationship between the friction factor and the Reynolds number which correlates with the Poiseuille relationship in Equation 2.2.2. In the turbulent flow region, the relationship is a function of the roughness of the tube surface. The transitional region is merely a shaded area on the diagram. Limited reliable data is available in this flow regime; however, efforts are being made to improve this.

In the high Reynolds numbers region (turbulent) the friction factor can be can computed using two different correlations. The Colebrook Equations (2.3.1) takes the roughness of the tube surface into account and it is the equation that the Moody chart is based on.

$$\frac{1}{\sqrt{f}} = -2.0\log\left(\frac{\epsilon/d}{3.7} + \frac{2.51}{Re_d\sqrt{f}}\right) \tag{2.3.1}$$

The Blasius Equation (2.3.2) was developed by H. Blasius in 1911 and was the first correlation to describe friction factor in turbulent flow, in terms of Reynolds number.

$$f = 0.316 Re_d^{-0.25} \tag{2.3.2}$$

The equation is valid for Reynolds numbers between 4 000 and 100 000 [23].

Efforts have been made to improve the accuracy of the Blasius and other related friction factor equations. Fang and Xhou [24] formulated two new equations for single phase tube flow. These equations improved upon the Blasius equation by better defining the Reynolds number ranges. With one equation for flow in smooth tubes and one for rough tubes, both equations boast a mean absolute relative error of 0.022%. As this accuracy exceeds that of the measuring instrumentation used in this study, only the original Blasius equation will be considered for validation purposes.

2.3.2. Entrance Region

2.3.2.1. Boundary Layer

Ludwig Prandtl, the engineer who defined the Prandtl number, published a theory on the boundary layer that occurs when fluid flows over a surface. He noticed that 'fluid flows with small viscosity, such as water flows and airflows, can be divided into a thin viscous layer, or boundary layer, near solid surfaces and interfaces and patched onto a nearly inviscid outer layer' [20].

In other words, the layer of fluid flowing adjacent to a solid surface is the region where the viscous effects of the fluid flow are significant, and this layer is called the boundary layer. The theory has proved very influential in the field of fluid mechanics as it is an important tool used for analysing flow. According to Prandtl's theory, the layer onto which the boundary layer is 'patched' is considered inviscid, thus the Bernoulli and Euler equations apply in that region. One of the other consequences of the boundary layer is the no-slip condition. Due to the viscous effects of the boundary layer, the fluid in direct contact with the solid surface 'sticks' to the surface and thus no slip occurs. This allows for the assumption that the velocity of the fluid at the surface is zero. Since the fluid is motionless next to the surface, the heat transfer from the solid surface to the fluid is by convection only.

The no-slip condition means that when a fluid enters a tube the particles touching the tube walls will have no velocity. This causes a dragging effect on all of the neighbouring particles so that the velocity increases from the wall to the centre of the tube. Visually this creates a conical velocity gradient inside the tube. The dragging effect mentioned is also called the region of viscous shearing. A hypothetical boundary, called the boundary layer, separates the region where these viscous effects are felt and the region where the irrotational velocity core is unaffected by them. The boundary layer grows until it reaches the centre of the tube and the conical velocity profile forms. The flow is then said to be hydrodynamically fully developed.

A similar theory can be applied to the thermal boundary layer, where the fluid temperature next to the walls will be the same as the wall temperature. This initiates convective heat transfer throughout the fluid. Once the heat transfer has propagated throughout the fluid and the thermal boundary layer has reached the centre of the tube, then the fluid is said to be thermally fully developed. The distance it takes the fluid to become fully developed is called the entrance length.

In turbulent flow, due to the chaotic nature of the flow, mixing of the fluid occurs more than in laminar flow and the hydrodynamic and thermal entrance lengths are approximately equal. They are taken as 10 times the inside diameter of the tube. In laminar flow the entry lengths are calculated using Equations 2.3.3 and 2.3.4 [21].

$$L_h = 0.05ReD \tag{2.3.3}$$

$$L_t = 0.05RePrD \tag{2.3.4}$$

2.3.2.2. Inlet Geometry Effects

As previously mentioned, the expected range where turbulent flow occurs is 2 300 <Re< 10 000. However this was developed for flow in tubes that have very steady flow and a rounded entrance. The inlet geometries of the tubes affect when the transitional region occurs in the flow and also when the flow becomes fully developed. Disturbances introduced by the inlet will also alter the friction coefficient.

Professor Afshin Ghajar and his co-workers were the first to conduct any experimentation into the affects that the inlet geometry has on the flow within horizontal tubes in the transitional flow regime. This is discussed in more detail in section 2.4.3.

2.3.3. Secondary Flow

Primary flows occur in the direction in which the bulk of the fluid is moving. In tubes this will be parallel to the tube walls. Secondary flow is the component of flow that moves perpendicular to this. Changes in geometry, such as a bend in the tube, will cause secondary flow. Upstream disturbances can also produce this phenomenon. However in straight, smooth tubes it can also be induced by the effect of drag on the boundary layer of fluid next to the tube walls.

2.3.4. Maldistribution

As its name suggests, maldistribution is the uneven or misaligned distribution of flow. The geometry of the heat exchanger can induce maldistribution into the flow. In a reverse manifold situation, such as is encountered in a shell and tube heat exchanger a portion of the tubes will always experience an uneven flow. This can be predicted using a statistical probability distribution plot. In a shell and tube heat exchanger mainly gross geometric maldistribution occurs. Other types of geometrically induced flow distributions include passage-to-passage maldistribution. However this is only significant in very compact heat exchangers. Gross flow maldistribution occurs due to blockages or fouling of the tubes. It can also be induced with a bad header design. A well designed header should deliver a uniform flow and there should be a minimal pressure drop in the header [25].

The operating conditions of the heat exchanger can also induce maldistribution. Viscosity induced maldistribution is caused by variations in the viscosity of the fluid within the tubes. If different tubes have different heat transfer rates then the viscosity in these tubes will also differ. This will lead to an uneven flow rate. This is most likely to occur when there is more than one type of fluid, also if the more viscous fluid is being cooled [4].

The skin friction coefficient is affected by the viscous drag in the boundary layer of the flow along the wall of the tube. In laminar flow, the skin friction coefficient is proportional to the fluid velocity, therefore maldistribution effects will be seen in this flow regime. In the turbulent flow regime the skin friction coefficient is proportional to the quarter root of the fluid viscosity [25].

Self-induced maldistribution is not only driven by viscosity but also by density and phase change within the fluid flow. As these properties change along the length of the tubes the flow becomes unevenly distributed and this can cause a disturbance in the flow.

2.4. Fluid Flow Regimes

2.4.1. Laminar Flow

As discussed in Section 2.2 the Reynolds number is used to distinguish the flow regime. Laminar flow occurs at low Reynolds numbers and can be described as smooth, steady flow, where the velocity profile of the flow is parabolic. All natural disturbances in the flow are damped out very quickly. The smooth flow results in a lower friction factor and therefore a smaller pressure drop. Laminar flow in circular, smooth tubes usually occurs at Reynolds numbers of less than 2 300 [21], and this value is referred to as the critical Reynolds number.

Due to the smoothness of the flow, downstream disturbances in laminar tube flow are felt upstream, before the disturbance is reached. This is referred to as the" far-seeing abilities" of laminar flow. Therefore tubes with different outlet resistances will experience different pressure drops across the entire length of the tube, upstream from these disturbances [20].

2.4.2. Turbulent Flow

Agitated and chaotic flow is known as turbulent flow and occurs in tubes at Reynolds numbers higher than 10 000 [21]. The velocity within the flow fluctuates randomly. The increased friction in the flow, caused by the fluctuations also leads to an increased pressure drop.

2.4.3. Transitional Flow

Transitional flow occurs somewhere in the range between the critical Reynolds number and Reynolds equal to 10 000. This is only valid for flow in smooth, round ducts. As summarised by Meyer [2], when transitional flow occurs, the flow changes in the following ways:

- Local velocities and pressures within the flow fluctuate
- The flow becomes more uniform as turbulence becomes more dominant. This is due to the mixing the turbulent flow creates.
- The friction factors are proportional to $Re^{-\frac{1}{2}}$ in laminar flow but the proportion transitions to $Re^{-\frac{1}{5}}$ with the onset of turbulence.

It is generally accepted that at a Reynolds number of 2 300 the flow will be fully laminar and at 10 000 it will be fully turbulent. In the range in between it is intermittently laminar and turbulent with a range of fully transitional flow. The occurrence of the intermittent laminar and turbulent regimes is determined by the intermittency factor. The factor is zero at the critical Reynolds number, where the flow is fully laminar and it increases, downstream to a maximum where the flow is fully turbulent. It has also been shown that the factor increases from the centreline of the tube towards the tube walls and becomes constant at about 20% of the boundary layer thickness [26].

2.4.3.1. Pressure Drop in Smooth Tubes

Work was conducted by Ghajar and his colleagues [7] [5] [8] to create a pressure drop database in the transitional flow regime, for flow in smooth horizontal tubes. The three major types of tube inlets are the re-entrant, the square-edged and the bell-mouth.

Ghajar and Madon [7] experimentally studied the effects that the inlet geometry has on the transitional fluid flow in horizontal smooth tubes by analysing adiabatic pressure drop. Their experimental setup consisted of a calming section, followed by an inlet section. The purpose of the calming section is to directionalise the flow that enters the test section. This ensures that the velocity is evenly distributed at the inlet and that any disturbances are removed. This is vital as disturbances cause transition to occur earlier and only the effect of the inlet disturbance is of interest. The inlet was interchangeable for the different inlet geometries being studied. The inlet section lead into a 6.1 m long seamless, stainless steel tube with an inside diameter of 15.8 mm. The working fluid used was water mixed with ethylene glycol.

Table 2.1 summarises the transitional regime results found in Ghajar and Madon's study. The bell-mouth entrance causes the least amount of flow disturbance so transitional flow occurs much later than the square-edged or re-entrant geometries. The re-entrant geometry causes the most disturbances and forces the turbulent regime to start at a lower Reynolds number. It is therefore clear that the inlet causes a significant disturbance on the flow in the tubes and this affects when transition will occur.

Table 2.1: Summary of transition ranges, based on adiabatic pressure drop data [7].

Re-entrant	Square-edged	Bell-mouthed
1 980 < *Re* < 2 600	2 070 < *Re* < 2 840	2 125 < *Re* < 3 200

The following correlation was formulated to describe the friction coefficient curve that forms in transition. Table 2.2 summarises the necessary coefficients for this correlation.

$$Cf = a + bRe + cRe^2 \tag{2.2.7}$$

Table 2.2: Constants for the adiabatic friction factor correlation.

Inlet geometry	a	b	c
Re-entrant	-9.88×10^{-3}	1.15×10^{-5}	-1.29×10^{-9}
Square-edged	-2.56×10^{-2}	2.49×10^{-5}	-4.25×10^{-9}
Bell-mouth	-8.03×10^{-3}	1.05×10^{-5}	-1.47×10^{-9}

In 1997 Ghajar and Tam [5] conducted further investigations on a similar test bench to study the effect that heating has on the pressure drop. The tubes were heated using an induced current, supplied by an arc welder. Table 2.3 outlines the ranges of Reynolds numbers at various heat fluxes where transitional flow is expected to occur. With the application of the constant heat flux boundary condition the onset of transition is delayed. These results differ from the original results published by Ghajar and Madon, however the delayed transition phenomenon is not discussed by the authors.

Table 2.3: Summary of transitional flow ranges for different inlet geometries and heat fluxes [5].

Heat Flux (kW/m^2)	Re-entrant	Square-edged	Bell-mouthed
0	2870 to 3500	3110 to 3700	5100 to 6100
3	3060 to 3890	3500 to 4180	5930 to 8730
8	3350 to 4960	3860 to 5200	6480 to 9110
16	4090 to 5940	4450 to 6430	7320 to 9560

Transition into the transitional flow regime occurs at the Reynolds number where a sharp change in the friction coefficient occurs. As was found for the adiabatic results [7], the bell-mouth entrance causes the least amount of flow disturbance and the re-entrant causes the most. This corresponds to the start of transition, with the increased disturbance causing transition to start sooner.

Tam *et al.* [8] later revised these experiments to investigate the effect of inlet geometry on the entrance and fully developed friction factor for laminar and transitional flow. For the square-edged inlet, the transitional flow range is 2 222 <Re< 3 588. The experiments were conducted using glycol-ethylene and water mixture as the working fluid and 6 m long tubes with an inside diameter of 14.8 mm. The prevailing conclusion from all this research is that creating disturbances at the inlet of the tubes causes transition to start earlier.

Similar experiments were later conducted by Meyer and Olivier. Their research was aimed at finding the effect that the inlet geometry has on transitional flow for tubes at a constant surface temperature, rather than constant wall flux. A constant heat flux on the tube is much easier to engineer in the experimental setup. However a constant surface temperature is a boundary condition that is more likely to occur in evaporation and condensation applications and therefore the research has important uses for industries such as; solar, nuclear, aerospace and HVAC. To achieve this boundary condition a tube-in-tube setup was created with fluid flow in the annulus to keep the wall of the inner tube at a constant temperature. The fluid in the annulus was kept at a high velocity and the size of the annulus was designed so that the flow was turbulent. This was to ensure that the thermal resistance of the fluid was much smaller in comparison to the flow in the inner tube. The inner tube was used as the test section and water was used as the working fluid.

Another difference in the tests was that the working fluid in the test section was being cooled instead of heated. Cooling fluid was shown to have different viscous effects by Petukhov [27]. Petukhov found that the viscosity near the walls is higher for a fluid that is being cooled down, rather than being heated. The necessity to investigate this further is clear as the higher viscosity at the walls should have an effect on the pressure drop in the tubes.

Meyer and Olivier tested four different inlet geometries. The first three: re-entrant, square-edged and bell-mouthed were used by Ghajar in his tests. A forth entrance type, the hydrodynamic, fully developed section was a new inlet that Meyer investigated. This entrance type was used so as to investigate the effect of a fully developed velocity profile at the entrance.

It was discovered that the square-edged entrance delays transition more than the re-entrant geometry and that the bell-mouth delays it the most. This agrees with Ghajar's [5] results: the larger the disturbance the inlet creates, the lower the critical Reynolds number. The difference in the results is due to the fact that Ghajar heated his test fluid. Also he only took measurements in the fully-developed section of his test section, significantly far downstream. However Meyer took measurements over the length of the tube, including the developing section.

The re-entrant inlet has a very small difference in results between the fully developed and developing adiabatic friction factors. In Meyer's results, the square-edged and bell-mouth inlets notably delay the start of transitional flow. The solid markers show the 15.88mm diameter tubes and the empty markers are for the 19.02mm tubes. For the bell-mouth inlet there is a large difference in the start of transition for the two different tube diameters. For the smaller diameter tube transition starts at around Reynolds numbers of 7 000, and 12 000, for the larger tube.

Overall, it can be concluded that in the laminar and turbulent flow regimes, in smooth tubes, the shape of the inlet does not influence the friction factor. However, in the transitional flow regime, these inlet shapes influence the friction factor, with the start of transition appearing earlier with the presence of a greater inlet disturbance.

2.4.3.2. Pressure Drop in Enhanced Tubes

In an attempt to increase the performance of heat exchanger units, the tubes are often enhanced in a variety of ways. The goal of enhancement is to increase the available heat transfer area on the inside of the tube. This can be achieved by adding fins, machining ridging or inserting tape into the tubes. These augmentations can be added lineally or helically wound within the tube.

Meyer and Olivier [11] again conducted experiments using the same test setup as before: four different inlet geometries on horizontal tubes. However this time they investigated the effects of enhancing the tubes with helical fins. Two different tube diameters were tested again; each with one case of 25 fins at 18˚ and one case of 35 fins at 27˚.

The results showed that the adiabatic friction factors for the enhanced tube are higher than that of the smooth tube results. Transition also appears to start earlier than in smooth tubes. This was expected as the tube enhancement adds disturbance to the flow.

Meyer found that although the tubes had different diameters, the results were the same if the tubes had the same number of fins and the same helix angle. A secondary transitional region appears in the region of 3 000 <Re< 10 000. The fins used in the enhancement cause the fluid in the tubes to rotate. This swirl in the flow is thought to induce a second spike in the friction factor [11].

2.4.3.3. Pressure Drop in Developing Flow

An investigation into developing flow in tubes was conducted by Everts [16]. It was observed that previous studies had either been conducted for fully developed flow [11] or the state of the flow had not been defined and pressure drop measurements were conducted over non-specific lengths [7]. Investigating pressure drop in developing flow is necessary to better understanding the transitional flow regime.

Everts conducted experiments on a test bench consisting of a 2.03 m long, smooth copper tube with an inner diameter of 11.52 mm. At the inlet was a calming section, similar to that used by Ghajar [7]. The study only investigated the square-edged inlet shape. Pressure drop measurements were taken over the length of the tube at a characteristic length of 2 m.

Both adiabatic and diabatic tests were conducted at Reynolds numbers between 500 and 10 000. Diabatic tests were run at heat fluxes of 6.5, 8 and 9.5 kW/m^2. The friction factors were measured at an uncertainty of 1% to 17%. Everts defined five different flow regimes so as to better describe developing flow: laminar, developing laminar, transitional, low-Reynolds-number-end and turbulent flow.

The laminar region yielded results similar to those found in literature for fully developed flow, whereas the developing laminar region differed. Secondary flow effects were found to play a role, causing the diabatic friction factors to increase in the laminar flow region. In the turbulent regime the heat flux had negligible effect on the friction factors.

In the transitional flow regime the results for the adiabatic pressure drop were similar to those found in previous studies. The friction factor curve exhibited the same basic shape, but a steeper gradient than previously seen. Everts concluded that the bandwidth of transition increases as the flow becomes more developed.

2.4.3.4. Pressure Drop in Nanofuids

With the trend to compact the size of computing and communications technology, the most common problem encountered is the issue of decreasing the size of the thermal management system without diminishing the cooling capacity. Nanofluids are therefore used in these circumstances. The addition of solid particles to water has been shown to increase its thermal conductivity by 5 000 times. With this massive increase in thermal conductivity it was speculated that using nanofluids in heat exchangers may have the same effect of improving their efficiency. Meyer *et al.* [14] investigated the effect that multi-walled carbon nanotubes have on the transitional flow in tubes.

The test section consisted of a copper tube with an internal diameter of 5.16 mm. The experiments were conducted at a single heat flux of 13 kW/m^2, and for three different concentrates of nanofluids: 0.33%, 0.75% and 1%. The nano particles used had an internal diameter of 3-5 nm and a length of 10-30 µm.

Adiabatic pressure drops were measured in a range of 1 000 to 8 000 Reynolds number. In the laminar flow regime the friction factor results were 3.3% lower than those predicted by previous literature. The correlation to theory was good in the turbulent flow regime. In transitional flow regime the friction factor curve was similar to those predicted by theory, but the bandwidth of the transition region was much smaller, with transition occurring for the range 3 100 <Re< 3 200. Overall, neither the friction factor nor the heat transfer capabilities were improved by the nanofluid. It served only to increase the viscosity of the working fluid such that the nanofluid was ineffectual.

2.4.3.5. Pressure Drop in Mini- and Microtubes

As mentioned in the section above (2.4.3.4) there is an increasing trend to miniaturise new technologies and the need for mini- and micro- heat exchangers is growing. Much study is being dedicated to the flow in these minitubes due to their usefulness in technologies such as fuel cells, artificial blood vessels and various sensors. However, the transitional flow in these minitubes has been neglected. Ghajar *et al*. sought to remedy this in an experimental investigation they published in 2010 [28].

The experiments were conducted for 12 different test tube sizes, with minitubes ranging from 2 083 to 1 372 µm and microtubes, from 1 372 to 337 µm. Ghajar *et al.* found that the adiabatic pressure drop in the transitional flow regime, for minitubes, was similar to that found in previous studies for macrotubes. However, in the micro-sized tubes, the decrease in diameter and the increase in relative roughness altered the friction factor in the laminar and transitional flow regimes. With each decrease in diameter the onset of transition was delayed. For diameters between 559 and 337 µm the friction factor profile in the laminar and transitional regime was significantly altered, with the friction factor being much higher at the low flow rates. The bandwidth of the transitional flow regime became narrower with each decrease in diameter.

2.5. Summary and Conclusions

This chapter served as a summary of a basic terminology, a few fundamental concepts and the different types of fluid flow, necessary to understanding the work in this report. It also provided a review of previous work conducted into the adiabatic pressure drop in the transitional flow regime.

Ghajar and his colleagues investigated adiabatic pressure drop over the full length of smooth tubes, using glycol ethylene as the working fluid. Meyer and his colleagues took average pressure drop readings across smooth tubes with water as the working fluid. Both Meyer and Ghajar tested the effect of different inlet shapes. In smooth tubes, the onset of transitional flow was made earlier for disturbances at the inlet of the flow. Therefore inlet shapes that caused greater disturbance to the flow, caused transition to start at a lower Reynolds number.

A study was conducted by Meyer and his colleagues into the effects of tubes enhanced with helically coiled fins. They found that the disturbances cause by the fins had the effect to hasten the start of transitional flow in the tubes. Meyer also investigated the effects of heat exchangers with nanofluids are the working fluid. However, this was found to have no effect on the friction factor.

Everts investigated the pressure drop in smooth tubes for developing flow. Similar adiabatic friction factors were found but with a smaller transitional band of flow. It was concluded that the bandwidth of transitional flow increases as the flow becomes more developed.

Microtube flow was investigated by Ghajar and his colleagues. It was found that the decrease in diameter and relative increase in surface roughness had a very small influence on the friction factor. However, after the diameter became smaller than 1 372 µm, the shape of the friction factor curve was much altered and the pressure drops in laminar and transitional flow were higher. It was also noted that the bandwidth of the transitional flow regime became smaller with a decrease in diameter.

Overall, the transitional flow regime had been investigated for single smooth tubes, smooth tubes with different inlet shapes, enhanced tubes and microtubes but no investigation into multiple tube entrances has been done.

3. Experimental Design and Methodology

3.1. Introduction

The aim of this chapter is to describe the experimental setup used for taking pressure drop measurements making use of two different types of test sections. The one test section consisting of a single tube being used for validation purposes and the second test section consisting of three tubes in parallel. An overview is provided of the experimental setup, the calming section, and the two different types of test sections that were used for experiments. The instrumentation used is discussed, as well as the data reduction method, with aim to determine the friction factors as a function of Reynolds number for the two types of test sections. The experimental procedure is discussed and an uncertainty analysis is performed with the purpose of determining the uncertainties of the friction factors and Reynolds numbers. The chapter is concluded with a short summary.

3.2. Experimental Setup

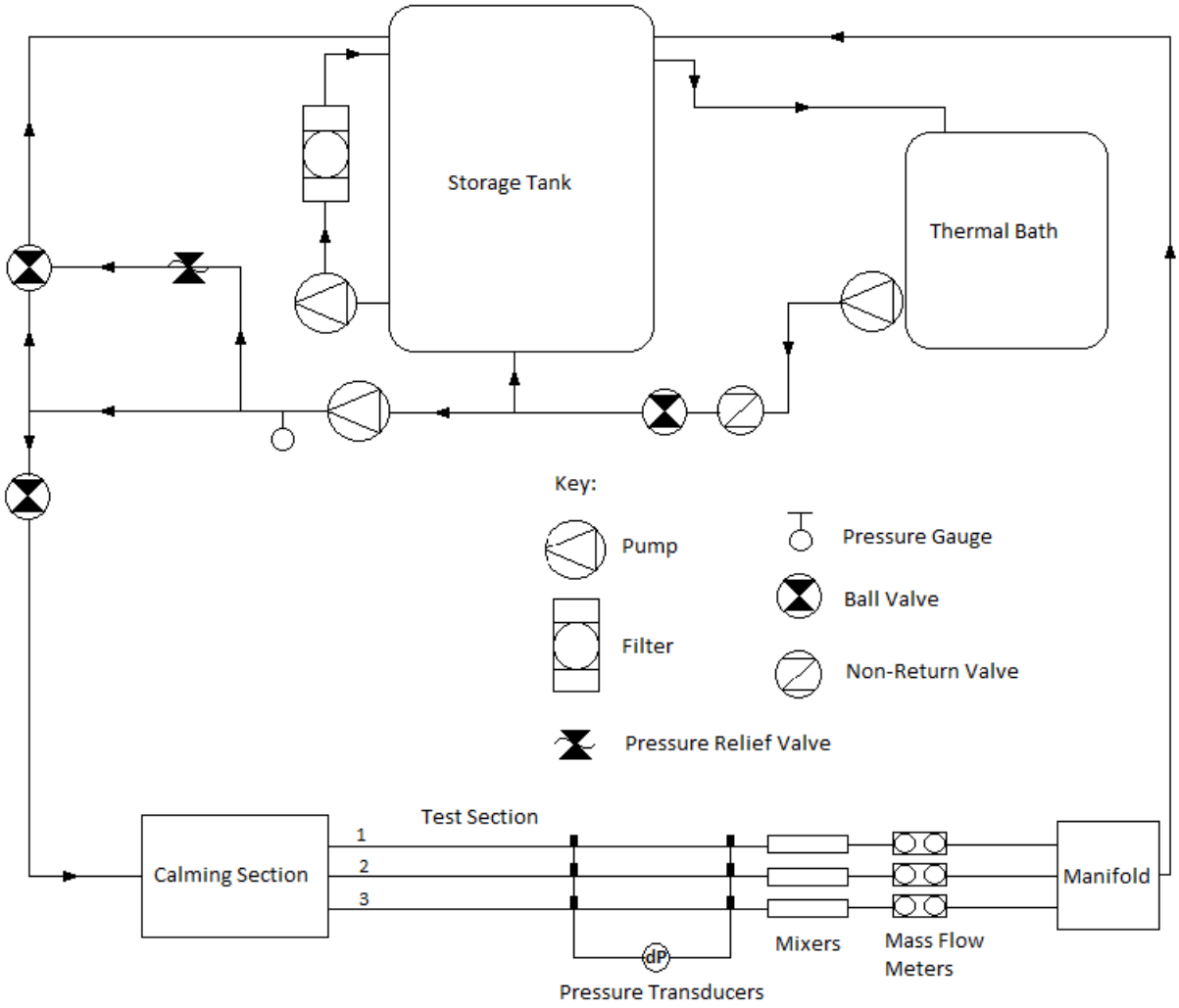

Figure 3.1: Schematic of the experimental setup that was used to circulate water and take pressure drop measurements on a three tube test section. In this schematic the three tube test setup is shown, but the system was designed such that a single tube setup could be inserted in place of the three tube setup.

Figure 3.1 shows the closed loop system that was used to circulate water, the chosen working fluid. The water was pumped from a thermal bath to the test section and returned to a 1 000 ℓ storage tank. The capacity of the thermal bath was sufficient to maintain the water at the required temperature. The function of the additional storage tank was to improve the stability of the system and function as a possible buffer against small temperature variations.

This water circulation process was electronically controlled by a positive displacement pump with a maximum flow rate of 421.1 ℓ/hr. The water in the system was maintained in the storage tank and thermal bath, at 22.5°C (±0.1^{o}C) by the thermal bath, which had a maximum cooling capacity of 900 W.

A bypass system was included after the pump. It consisted of two ball valves: one before the test section, used as a flow control valve and one between the storage tank and the pump, used as a bypass valve. The system pump created small pulsations in the flow at low pump speeds, due to low backpressure. The bypass system was then used to increase the backpressure by keeping the bypass valve partially closed and operating the control valve so that the desired mass flow rate was always produced when the pump head was turning close to the maximum revolutions per minute. This minimized the pulsations in the flow, which were monitored at the mass flow meters.

A pressure relief valve was installed after the pump so that if the system pressure exceeded the maximum operating pressure of the pump, the water would immediately feed back into the storage tank. The pressure relief valve was calibrated to 350 kPa. This also provided a safety mechanism that protected the calming section from over pressurizing and cracking.

The experimental bench and test setups were built in an enclosed and temperature controlled laboratory. All experiments were conducted with the ambient temperature at approximately 23^{o}C.

3.3. Calming Section

A calming section (Figure 3.2) was included at the inlet of the test section to directionalise the flow that enters the tubes. The design was based off the one used by Ghajar [5-8, 21] and Meyer [9, 11, 16] and whose function was to create a uniform inlet velocity profile. The contraction ratio, which is the cross-sectional area of the calming section to the cross-sectional area of the tube inlet for these studies were approximately 126.

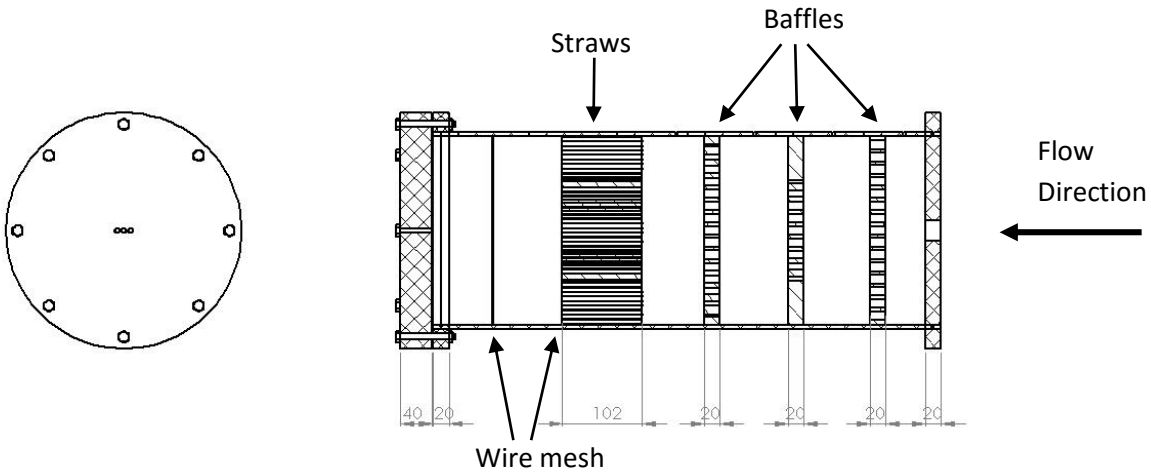

Figure 3.2: Illustration of the calming section used in the experiments, based on the work of Ghajar and Madon [7]. Dimensions are in mm. The calming section is shown here with the three tube test section inlet. A single tube inlet header was used for the single tube test section.

The same contraction ratio was used in this study. However, the tube inlet area used was not the cross-sectional area of the three tubes but the inlet area of disturbances/flow. This was based on using one "effective diameter of disturbances" which was the sum off all three tubes plus the pitch distances in between as shown in Figure 3.3. This was a very conservative approach to ensure that the contraction ratio should not influence the results. The calming section outer diameter of 250 mm was selected to ensure a contraction ratio of approximately 120. As the same calming section was used for both the single-tube test section and the triple-tube test section, the contraction ratio for the single-tube was 1 736. The minimum contraction ratio used for both the single-tube test section and the three-tube test section was thus 120.

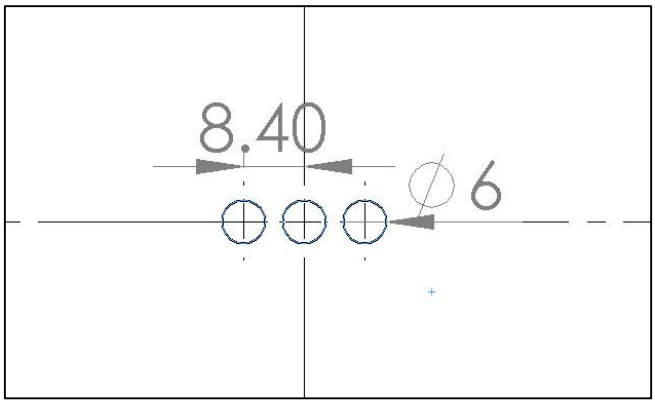

Figure 3.3: Schematic showing the pitch spacing of the three tubes in this study, and thus the effective area of disturbance.

Baffles inside the calming section body were used to straighten the flow. Three Perspex porous plates were used with a 20 mm thickness. Holes with a diameter of 11 mm were bored in a regular pattern, creating a plate with an open air ratio of 0.3088.

Plastic straws (inner diameter of 0.57 mm and 102 mm long) were tightly packed together and sandwiched between two stainless steel mesh screens. A single mesh screen was included just before the exit of the calming section. A stainless steel mesh with a strand diameter of 0.3 mm, mesh width of 1.4 mm and open air ratio of 0.65 was used.

Holes with a diameter of 3.175 mm were drilled into the top of the 600 mm calming section body to allow for bleeding points and for a PT100 probe. The probe was used to measure the average inlet temperature of the water. Screw-in hydraulic fittings were used to bleed the air out of the calming section as it filled up. The calming section was insulated with 32 mm thick insulation material with a thermal conductivity of 0.036 W/m.K, to minimize heat losses to the environment.

3.4. Test Section

A schematic of the three tube test section is shown in Figure 3.4. The tubes are labelled “Tube 1”, “Tube 2” and “Tube 3”, and will be referred to by these labels for the rest of the study. “Tube 2” is thus the tube in centre. The tubes used in the two test sections were seamless, stainless steel tubes (316L), with measured lengths of 6.000 m (±1 mm), which were measured using a measuring tape with a 1 mm accuracy. The tubes had an outside diameter were 6 mm and an inner diameter of 3.97 mm. The inner diameter of the tubes were measured at the inlet and outlet using a split ball measuring instrument with an accuracy of 20 µm.

The tubes were attached to the calming section using an interchangeable acetyl header plate. Two different header plates were manufactured: one to accommodate the single tube only and another to accommodate three tubes in parallel, as is indicated schematically in Figure 3.4. The header plate for the three tubes arranged the tube inlet spacing in a tube pitch of 8.4 mm (1.4 mm times the outer diameter). In this study the first test section will be referred to as the “single tube test section” and the second as the “three tube test section”.

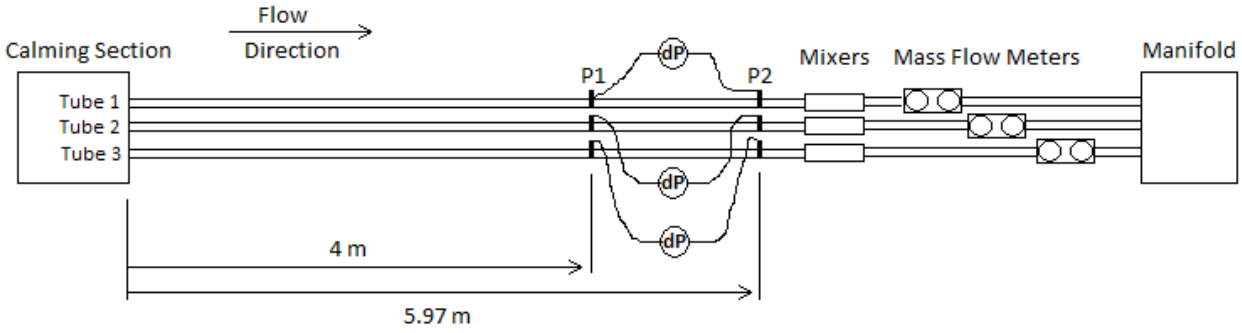

Figure 3.4: Illustration of the three tube test section that was used to measure the pressure drop across three tubes. For the single tube test setup the header plate of the calming section was replaced to accommodate the single tube.

To investigate the effect of many tubes in a shell-and-tube heat exchanger, and to investigate the influence of these multiple entrances on the transitional flow regime inside the tubes, only three tubes were selected for this study. This will give an indication of what happens in two dimensions (one plane of the heat exchanger).

Shell-and-tube heat exchangers traditionally have two types of tube arrangements, the in-line arrangement and the staggered arrangement [21]. Both of these are shown in Figure 3.4 and the three tubes for this study are circled in red for each. An arrangement of four and more tubes

would be a more accurate study of the inlet effects, as shown schematically in Figure 3.5. However, it would be more costly and time intensive to add new tubes. Thus, to keep the experiment simple and affordable, as well as to investigate the basic principles of multiple tube inlets, it was decided to test only the three tubes in this study. It is recommended that more tubes should be considered as a follow up study.

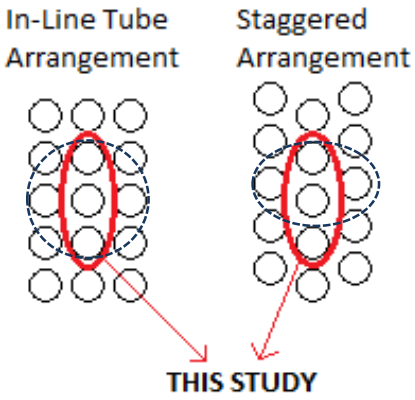

Figure 3.5: Schematic of the different tube bank arrangements found in shell-and-tube heat exchangers. The three tubes used in this study are circled. Circled in the dotted blue line are the potential arrangements that could be used for further studies.

The header plates were made from acetal with a low thermal conductivity (0.31 W/mK), to prevent axial heat loss. The tubes were press fitted into the header to form a square edged inlet and a glue, specific to the materials, was used to create a water-tight seal. Additional rubber gasket seals were used around each tube, on the outside of the header plate, and were held into pace by a Perspex saddle around the tubes. Care was taken to ensure that the tubes were smooth at the inlets, without any visible burs and that a square-edge was formed at the inlet such that there were no flow obstructions that could cause other inlet effects. A spirit level was also placed across the three tubes so as to align the inlets horizontally.

The pressure tap positions on the outside of the tubes were filed to create a flat surface on which the capillary tubes were silver soldered. The capillary tubes consisted of stainless steel tubes with an inner diameter of 1 mm and a height of 10 mm. The pressure taps were 0.4 mm holes drilled into the test tube, through the capillary tubes. This size tap diameter was chosen based on the recommended maximum size of 10% of the inner diameter of the test section [29]. The inside of the tube was inspected visually for any burrs caused by the drilling of the pressure taps. However due to the hardness of the stainless steel and the fineness of the drill bit no visible burrs formed at the pressure tap holes.

Hydraulic fittings with bush taps were fitted over the capillary tubes and thin nylon, flexible tube connected the other side of the fitting to the pressure transducers. The pressure drop distance between the two pressure taps was 1.97 m, and was located at the end of the tube, between 4 m and 5.97 m, as measured from the tube inlet.

The pressure drops were taken at this location since it was calculated that hydrodynamically, fully developed flow would occur at 3.2 m from the inlet, for adiabatic, laminar flow at a Reynolds number of 2 300. For diabatic, laminar flow it was calculated to occur at 2.7 m from the inlet. For the turbulent regime the flow will be fully developed in ten diameters or 39.7 mm. As this setup was also being used by others for diabatic studies in the laminar and transitional flow regimes the selected positioning of the pressure taps would ensure that the pressure drop results were always for fully developed flow.

The test sections were insulated using sheets of insulation material with a low thermal conductivity of 0.036 W/mK. The single tube test setup was surrounded by insulation with a thickness of 180 mm and the three tube test setup, with 268 mm of insulation material.

3.5. Mixers and Manifold

At the end of each tube a mixer was installed to ensure that the outlet temperatures were measured accurately. This was not essential for this specific study as the test section was not heated, but was used in other studies (as mentioned in Section 3.4). However, it was a convenient capability as it ensured that the fluid bulk temperature (which should not differ from inlet to outlet) could be measured very accurately. A schematic of one mixer is shown in Figure 3.6.

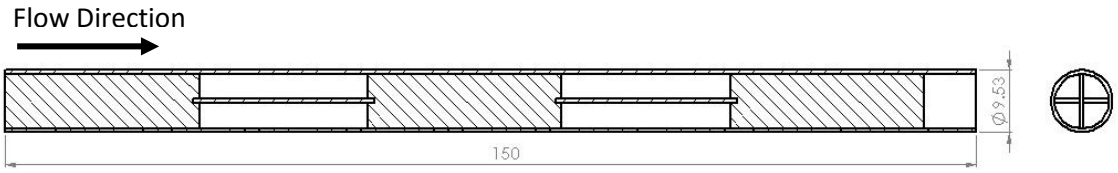

Figure 3.6: Illustration of the mixer used at the end of the test section to mix the flow before measuring the temperature. Dimensions are in mm.

Each mixer, shown in Figure 3.6, consisted of 9.52 mm copper tube with five copper plates, of length 25 mm, arranged in a cross-hatch orientation, each positioned 90^{o} from each other. Each time the plate orientation changed, the thermal boundary was split apart and caused the entire body of fluid to mix, ensuring a uniform temperature distribution. This design of the mixer was based on the work of Bakker *et al*. [30].

A manifold was implemented downstream of the mixers and the mass flow meters (Section 3.6.3). The manifold was built from the same Perspex tube that was used for the calming section, with an outer diameter of 250 mm. On the inlet side, a Perspex cap with three hose fittings, was used to attach the ends of the three tube test section. At the outlet, a similar Perspex cap with a single quick-couple fitting was used to attached the outlet hose, necessary to carry the test fluid back to the storage tank. The purpose of the manifold was twofold. Firstly to accumulate the fluid of all three tubes for the purpose of emptying it into the storage tank. Secondly, the manifold ensured that the resistance at the end of each tube was the same. The manifold was not used for the single tube setup.

3.6. Instrumentation

3.6.1. Pressure Transducers

Pressure transducers that measured differential pressures by means of interchangeable diaphragms, were used to find the pressure drop across the fully developed length of the tubes. Three DP15 transducers were chosen, each with three diaphragms with different full scale ranges, so that the pressure drops could be measured accurately across the full range of mass flow rates being tested. Thus for the three-tube test section, three different pressure transducers were used to measure the pressure drops at the same time.

The full scale range of the smallest diaphragms was 2.2 kPa and was used to measure Reynolds numbers from 800 to 2 100 with a resolution of 5.5 Pa. That equates to an accuracy of 1.8% at the lowest pressure drop. The mid-sized diaphragm was used for the ranges of 2 100 to 3 800, with a full scale value of 8.6 kPa, and the highest pressure differential range was measured by the 3-34, with a range up to 22 kPa.

The 2.2 kPa diaphragm was calibrated using an air-controlled Betz manometer with a full-scale range of 2.5 kPa. The other two diaphragms were calibrated using a hand-built water column. The pressure was measured using a Beta manometer with a full scale range of 50 kPa and a resolution of 100 Pa.

3.6.2. PT100 Measuring Probes

PT100 probes were used to measure the temperature of the water in the system. A single probe was inserted into the calming section to measure the bulk inlet water temperature. Three probes, one for each tube, were attached to the test setup after the mixers, by means of a tee-piece, such that the PT100 probe tip protruded fully into the flow.

As the experiments conducted for this study were all adiabatic, the PT100 probes were not essential but were present in the system for use in other diabatic tests performed on the same test rig. In this study the temperature measurements were used to measure the inlet and outlet bulk water temperature to ensure that there was negligible heat transfer from the surroundings into the test section.

The PT100s were calibrated using a DigiCal device, to an accuracy of 0.034^{o}C.

3.6.3. Flow Meters

Coriolis mass flow meters that could measure the full range of mass flow rates were placed at the outlet of each tube. The maximum capacity of each flow meter was 0.03 kg/s at 0.05% accuracy. For the three tube test section, a total of three meters were used in parallel, of the same manufacturer and model, to ensure that the mass flow rates of each tube were measured separately and simultaneously. This ensured that inlet maldistributions between the three tubes could be measured.

3.6.4. Data Acquisition and Logging System

A National Instruments Data Acquisition system was used to: control the pump speed via a current output card, log mass flow rates via a current input card and log pressure drops on SCXI 1308 (Signal Conditioning eXtensions for Instrumentation) cards. The NI Labview software was used to log the data and apply all of the calibration factors. Microsoft Excel and Matlab was further used to process the data.

3.7. Experimental Bench Setup

As was discussed in the scope of this master's study, the majority of the project duration was spent designing and building an experimental bench and a test setup. This experimental bench included all new, state of the art equipment and is now a part of the testing infrastructure at the University of Pretoria.

The fluid control section of the experimental bench is shown in Figure 3.7. The elements that can be seen in this image include: the storage tank, filter, storage tank circulation pump, calming section supply pump, pressure gauge and thermal bath, as well as all of the copper tubing, rubber hose and valves necessary to ensuring the fluid flow to and from the test bench. The inlet and outlet piping of this bench was equipped with quick-couple fittings to enable test sections to be removed and replaced as necessary.

The data acquisition system and other system instrumentation is shown in Figure 3.8 The flow meter transmitters, the demodulator for the pressure transducers, the data acquisition system and three power supplies are shown in this photograph. The power supplies are necessary for diabatic tests that can be run on the experimental bench.

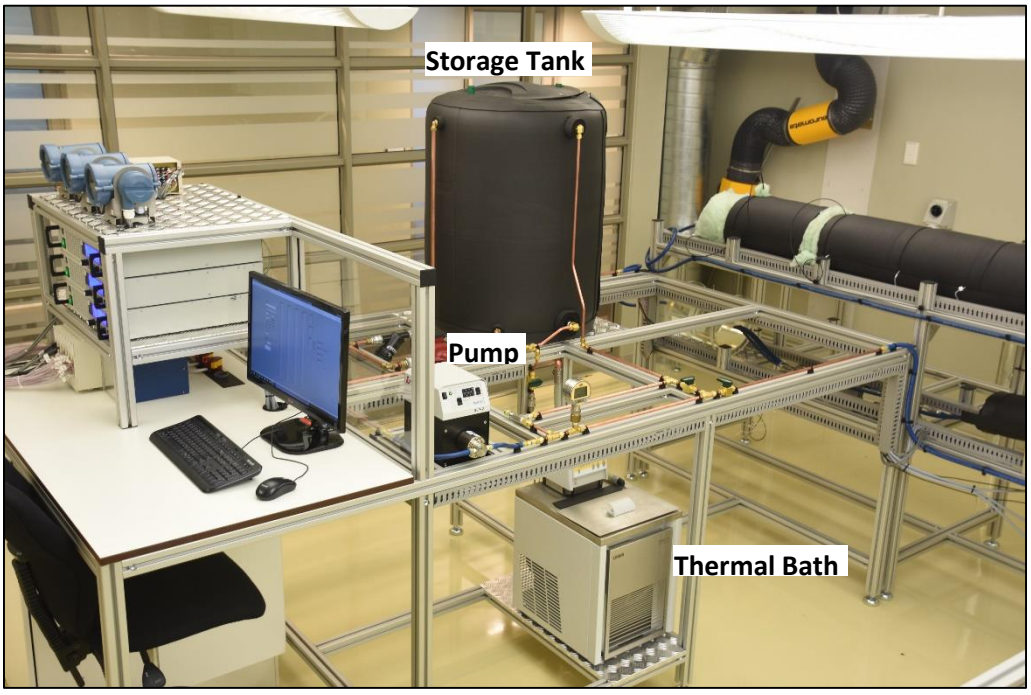

Figure 3.7: Photograph of the experimental bench, showcasing the storage tank, system pump, thermal bath and the water conduits.

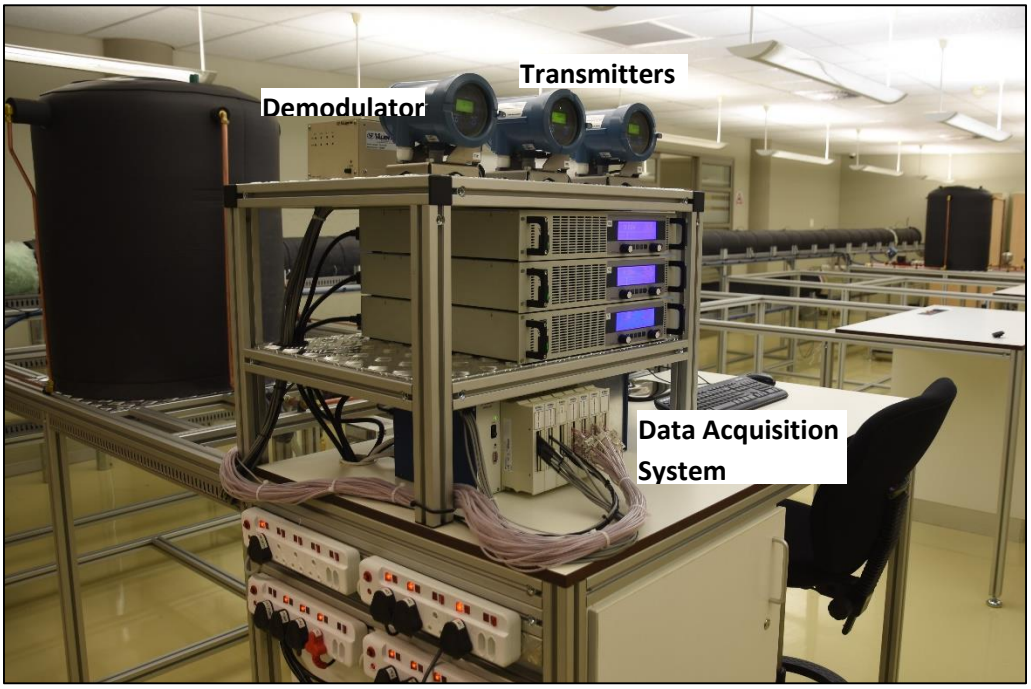

Figure 3.8: Photograph of the experimental bench, showcasing the instrumentation and data logging equipment.

The inlet calming section and outlet manifold are shown, respectively on Figure 3.9. The first image (a) shows the Perspex calming section, attached to the water circulatory system with a quick-couple fitting. The PT100 probe can be seen, screwed into the top of the body of the calming section. Downstream of the calming section, Armaflex insulation covers the three tubes. The same calming section is used for the single tube setup. The thermocouple wire protruding from the side of the insulation was used for temperature measurements conducted by other students during diabatic tests on the same setup. Figure 3.7(b) shows the outlet side of the three tube test section. Rubber hose, originating after the mixers and PT100 probes (covered by insulation), carries the water from the three tubes, through the mass flow meters, into the manifold, and then back into the storage tank on the experimental setup bench.

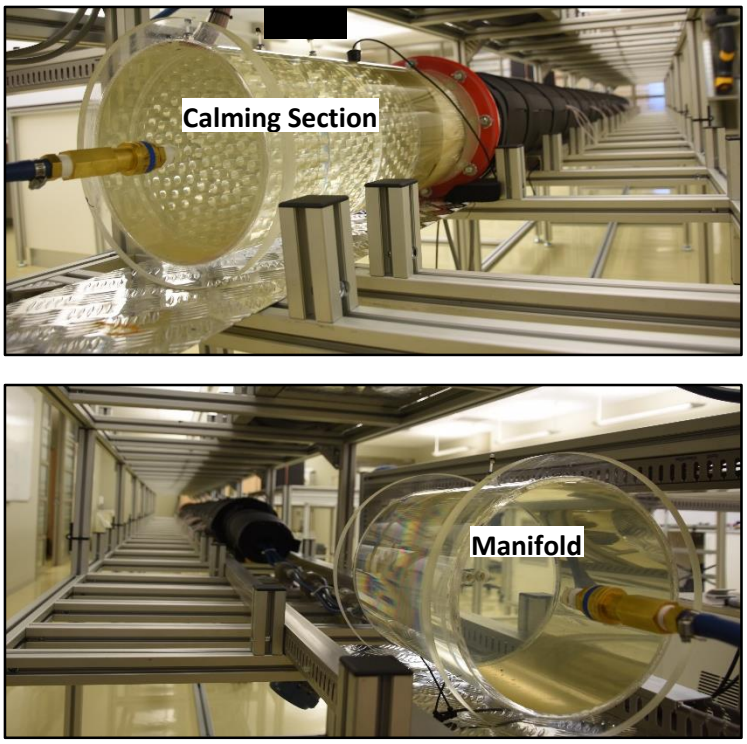

(a)

(b)

Figure 3.9 (a) Photograph of the calming section at the inlet of the three tube test section. The same calming section was used for the single tube test section. (b) Photograph of the equipment downstream of the three tube test section.

3.8. Data Reduction

The Reynolds numbers for the fluid flow in a single tube or each of the three tubes in parallel were determined as

$$Re = \frac{\dot{m}D}{\mu Ac} \tag{3.7.1}$$

Where: $\dot{m}$, was the measured mass flow rate of the water in a specific tube; D, the measured inner diameter of the tube, μ, the dynamic viscosity of the water, and A_c, the cross sectional area of the tube.

$$A_c = \frac{\pi}{4}D^2 \tag{3.7.2}$$

All the fluid properties (μ and ρ) were found using the thermophysical property correlations for water, as described by [31]. The properties were determined at the bulk temperature, T_b, determined from the two PT100's measuring the average water inlet, T_i, and outlet, T_o, temperatures.

$$T_b = \frac{T_i + T_o}{2} \tag{3.7.3}$$

The Darcy-Weisbach friction factor, f, was determined directly in terms of the measured pressure drops, ΔP, between the two pressure taps of each tube, measured mass flow rates, and measured distances between the two pressure taps, L_P, of each tube, which was 1.97 m.

$$f = \frac{2\Delta PD}{L_p \rho V^2} = \frac{\Delta P \rho D^5 \pi^2}{8\dot{m}^2 L_p} \tag{3.7.4}$$

In general, percentage errors in this study, were determined from the absolute difference between the measured and predicted results, with the measured as a reference value.

$$\%error = \frac{|measured - predicted|}{measured} \, x \, 100 \tag{3.7.5}$$

3.9. Experimental Procedure

Steady state conditions were considered to be reached when no significant fluctuations occurred in the measured pressure drops, mass flow rates and temperatures for a minimum period of five minutes. This is illustrated in Figure 3.9, where after 1 000 data points, or one minute, the significant fluctuations in the system had died out. Significant fluctuations are defined here as fluctuations that exceed the uncertainty band and expected noise range of the instrumentation. This data was recorded in the turbulent flow regime and it shows steady state conditions after six minutes. After the system was started for the first time it would take approximately 45 minutes before steady state conditions were reached. After measurements were obtained, small changes were made in the mass flow rates before the next set of measurements were made. Steady state conditions would then occur faster at approximately seven minutes for laminar flow, six minutes for turbulent, and 10 minutes in the transitional flow regime. It was also found that during all measurements the temperature difference between the inlet and outlet was negligible, and was less than the calculated uncertainty range of the PT100 probes.

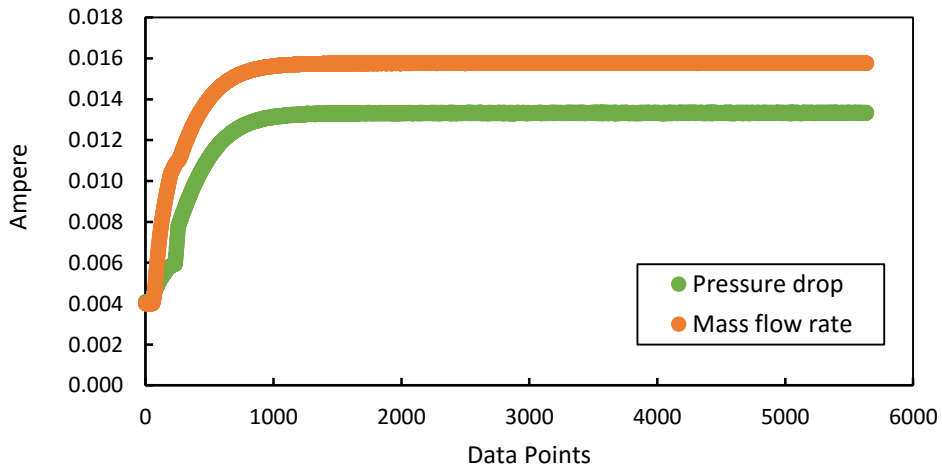

Figure 3.10: Graph illustrating the number of data points required to reach steady state in pressure drop and mass flow rate in the transitional flow regime. The total number of data points (6000) took 10 minutes to log.

In the turbulent and laminar flow regions, larger increments between different mass flow rates were chosen. However, in the transitional flow regime, finer increments were used so as to accurately map the results. According to Meyer and Olivier [9], the effects of hysteresis were negligible in the transitional flow regime. The flow rates were therefore mapped in increasing order, and then in decreasing order, with larger increments, as a check for repeatability.

As mentioned in Section 3.2, the supply and bypass valves were adjusted at each pump setting so as to increase the backpressure and minimise the effects of flow pulsations. For the three tube setup, an equal flow rate in all three tube was achieved by pumping water through the system at a high enough flow rate to give turbulent flow. In the turbulent flow regime the flow rates of each tube are independent of the inlet effects. An equal flow rate was achieved by clamping the downstream hoses until all of the flow rates measured within 0.05 l/hr of each other. This value was chosen as it is within the accuracy range of the mass flow meters. The clamps were located on the flexible rubber hose connecting the stainless steel tubes to the manifold.

Once steady conditions were reached at each flow rate, 200 data points were logged at a recording frequency of 10 Hz to obtain one measurement of each pressure drop, mass flow rate and temperature. The median value of these data points was used to obtain a single value for calculation purposes. Numerical trials were conducted at frequency between 1 and 10 Hz, with a number of data points collected between 20 and 2 000; and the same results were found. Therefore, the results were therefore independent of logging frequency and the number of data points collected.

3.10. Uncertainty Analysis

3.10.1. Instruments

The method described by Dunn [32] was used to perform an uncertainty analysis on the recorded data. First the accuracy and precision of the system instruments were calculated within a 95% confidence interval. This information is summarised in Table 3.1. The range and bias of the instruments were obtained from the manufacturer's specifications and the precision and accuracy was calculated using Everts [16] as a guideline.

Table 3.1: Accuracies of the instrumentation.

Instrument	Range	Resolution	Accuracy
Pressure Transducers			
22kPa	0 – 22 kPa	55 Pa	29.11 Pa
8.6kPa	0 – 8.6 kPa	21.5 Pa	5.13 Pa
2.2kPa	0 – 2.2 kPa	5.5 Pa	2.04 Pa
Flow Meter			
CMF010	0 – 108 l/hr	-	0.054 l/hr
PT100s			
All four PT100's	0 - 100^{o}C	-	0.034^{o}C

3.10.2. Fluid Properties

The thermophysical properties of the water were calculated using the correlations of Popiel and Wojtkowiak [31]. The uncertainties of each of these correlations is summarised in Table 3.2.

Table 3.2: Uncertainty of the fluid properties correlations.

Property	Density (kg/m^3)	Dynamic viscosity (kg/ms)
Uncertainty %	0.004	1

3.10.3. Reynolds Number and Friction Factor Uncertainties

The calculated uncertainties of Reynolds number and friction factors are summarised in Figure 3.11. The Reynolds number uncertainty was a function of density, flow velocity, viscosity and diameter of the tube. During the adiabatic tests the density and viscosity were almost constant. Therefore the only variable was the flow velocity, which increased with Reynolds number. The accuracy of the Reynolds number also increased as a function of increased flow rate. Thus it was found that the maximum uncertainty of the Reynolds number was less than 1.8% at a Reynolds number of 980 and decreased to 1.5% at a Reynolds number of 3 800. Thus in general it was concluded that the Reynolds number uncertainty was less than 2%.

The friction factor uncertainty was a function of pressure drop, diameter, density, fluid velocity and characteristic length. It was found that the variable influencing the friction factor most was fluid velocity. The uncertainty analysis calculations showed that the uncertainty of the friction factor was the highest at low Reynolds numbers and then decreased as the Reynolds numbers increased. At a Reynolds number of 980 the friction factor uncertainty was 0.9% and at a Reynolds number of 3 800 it was 0.7%. Thus in general it was concluded that the friction factor uncertainty was less than 1%.

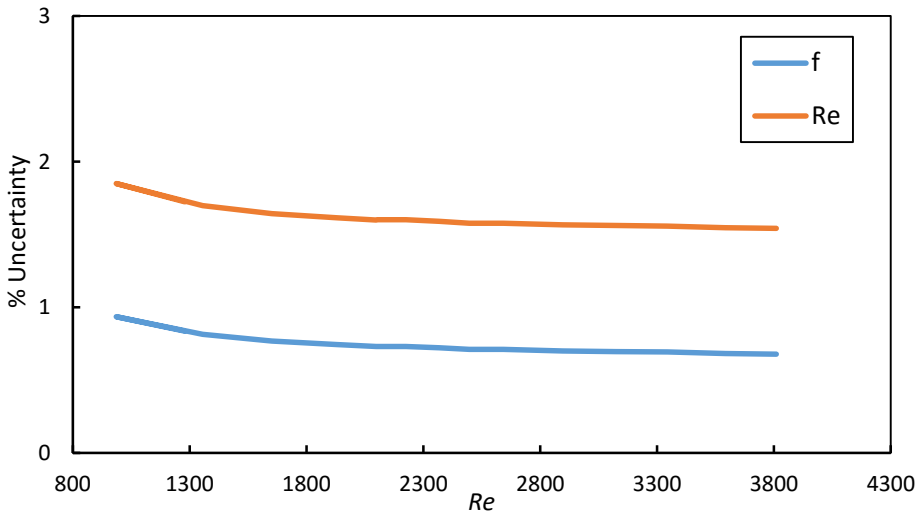

Figure 3.11: Uncertainty of Reynolds number and adiabatic friction factor as a function of Reynolds number.

3.11. Summary

This chapter consisted of a detailed explanation of the experimental setup, instrumentation, data reduction method, testing procedure and uncertainty analysis. The test setup consisted of two test sections. A single tube section with only one tube that was used for validation purposes, and a three-tube section with three 6 m long stainless steel tubes with an inner diameter of 3.97 mm.

Both the single tube and the three tube setups were alternatively attached at the inlet to a calming section with a square-edged inlet shape. Water was used as the working fluid and tests were conducted at Reynolds numbers of 700 to 5 100, with a finer resolution of measuring points in the transitional flow regime. The inlet and outlet temperatures were measured using PT100 probes.

The pressure drops were measured in the fully developed section between two pressure taps utilising a variety of carefully selected diaphragms. The entire test section between the temperature measuring probes was insulated to ensure that were was no heat transfer from or to the environment.

An uncertainty analysis was then performed on all of the data collected. The accuracies of all of the measuring equipment was determined or collected from the literature provided by the manufacturers. The calculated parameters were analysed using this accuracy information to determine the percentage uncertainty each calculated value had. The Reynolds number was found to have an uncertainty of less than 2%, while the friction factor uncertainty was less than 1%.

In this study only three adjacent tube inlets were investigated, with the tube arrangement in a single horizontal plane. These tube inlets were spaced at one pitch distance of 1.4 times the outer diameter. To expand on this study more inlet pitch distances should be considered. In future research into this field, other tube arrangements should be considered, with four or more tubes inlets, in two planes.

4. Experimental Validation

4.1. Introduction

This chapter discusses the validation of the experimental setup and the data reduction, by comparing the results to literature. In order to compare the experimental setup with previous work in literature, the three tubes in the system were replaced with a single tube. This single, stainless steel tube had the same dimensions as the other three and was prepared for experimentation in the same way. The pressure drop results from the single tube test were compared to the adiabatic friction factor results found in literature.

4.2. Adiabatic Friction Factors

Validation experiments were conducted on a test bench consisting of a single stainless steel tube. Pressure drop experiments were conducted across the last 1.97 m of the tube, where fully developed flow occurred. An initial test was conducted using the 22 kPa pressure transducer to gauge the system response and behaviour. Pressure drops for laminar, transitional and turbulent flow were found, with the experiments spanning a range of Reynolds numbers from 750 (laminar) to 9 300 (turbulent). A total of 23 useful data points were recorded. The friction factors were calculated and plotted as a function of Reynolds number, with both axes on a logarithmic scale, as illustrated in Figure 4.1.

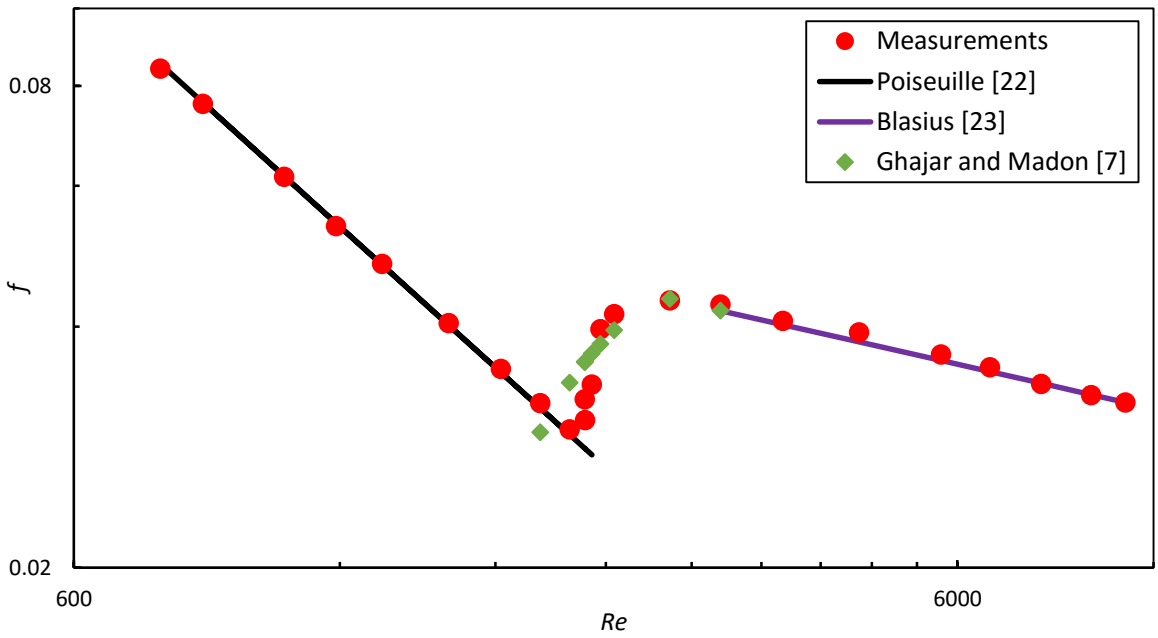

Figure 4.1: Adiabatic friction factors from initial testing, as a function of Reynolds number and validated against Poiseuille and Blasius theoretical models.

The initial results showed that in the laminar region the results corresponded well to those predicted by the Poiseuille equation [22] (Equation 2.2.2). Similarly, after a Reynolds number of 4 000 the Blasius equation [23] (Equation 2.3.2) was applicable. Due to the resolution of the 22 kPa diaphragm the effective accuracy increased as the pressure increased. Therefore, in this case the turbulent results were more accurate than those of the laminar.

On average the turbulent flow friction factor data was within 2% of the Blasius correlation, with a maximum of 3.3% difference in the lower flow rate end of the turbulent results. Figure 4.1 shows the experimental data was validated in the laminar and turbulent regions by existing theoretical models of friction factors for fluid flow in tubes. In the transitional region, the correlation found by Ghajar and Madon [7] was used to validate the experimental results. This correlation was described in Equation 2.2.7 and Table 2.2. The transitional region of flow fell within the ranges of 2 180 < *Re* < 2 830 which corresponds well to the results of Ghajar [7], as summarised in Table 2.1. Transition was found to start at a Reynolds number of 2 180 and compared well to the published value of 2 300 [21]. The transition point was identified by monitoring the gradient of the slope of the adiabatic friction factor. It was found that at this point the friction factor increased suddenly and the inclination of the gradient of the graph changed significantly. Therefore, this point was used as the onset of transition.

The initial tests showed that it was unnecessary to test at high Reynolds numbers as fully turbulent results could be found before a Reynolds number of 4 000. More accurate tests were then conducted in the range of 800 < *Re* < 4 000. The 22, 8.6 and 2.2 kPa pressure diaphragms were used to more accurately measure the pressure drop in the transitional region of flow. A total 53 data points were recorded and the results are shown in Figure 4.2. The experiments were initiated at a low flow rate and this was slowly increased until turbulent flow was achieved. This data was plotted as the 'Measured – increasing flow rate' points in the figure. The experiment was then repeated, beginning at the high flow rate and decreasing into the laminar flow regime. This data was plotted as the 'Measured – decreasing flow rate' results and it proves the repeatability of the experiments. Meyer and Olivier [9] investigated hysteresis effects in transitional flow and concluded that they were negligible. The results found in the conducted experiments supports their findings.

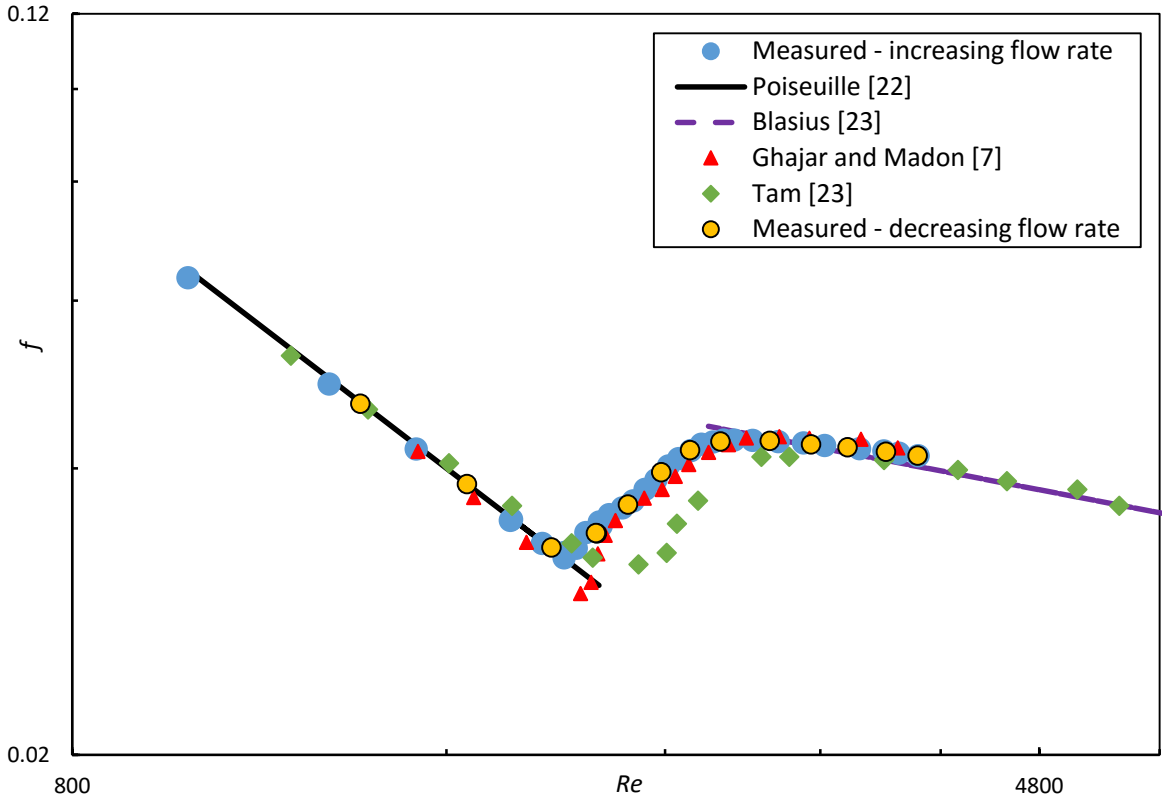

Figure 4.2: Adiabatic friction factor plotted against Reynolds number, illustrating the negligible hysteresis effects and the comparison to literature.

The results were again plotted against the Poiseuille and Blasius equations. The Blasius equation did not initially appear to correlate well to the data (2.7% error), however, the correlation of Blasius is only valid after a Reynolds number of 4 000 so the discrepancy can be neglected, as it was proved in the initial tests (Figure 4.1) that the turbulent data did correspond in the fully turbulent regime. In those experiments the error was 2% once the flow was fully turbulent.

The laminar region of flow the experimental data was compared to the Poiseuille correlation. On average the experimental data was within 1.5% of the correlation and had a maximum deviation of 3.8%. Therefore, there was a good correspondence between the theoretical data and the experimental data in the laminar and turbulent regimes of the testing.

The experimental data was also compared against the work of Ghajar and Madon [7] and that of Tam [8] in Figure 4.2. The adiabatic friction factors determined in the experiments were on average within 3.4% of Ghajar and Madon, and 9.8% of Tam in the turbulent regime. In both cases, the previous work was conducted with much larger test tubes. Transition was found to occur in the range 1 989 < *Re* < 2 726, and the onset of transition was identified to occur at a Reynolds number of 1 989. This transition point, which should be more accurate than the one identified in Figure 4.1, was also identified using the same methodology previously described.

Comparing this to the results of Ghajar and Madon (Table 2.1), the transitional range had the same width (a Reynolds number difference of 737) but started 4% earlier than predicted by Ghajar [7]. In Tam and Ghajar's experiments [7, 8] a glycol ethylene and water mixture was used as the working fluid with a much larger Prandtl number, and also the tube diameter was larger. The pressure drop measurements were also taken over the full length of the test section, and were not confined to the fully developed section only. In this study only fully developed pressure drops were measured.

In general, it can be concluded that the friction factor results as function of Reynolds number compared well with literature in the laminar and turbulent flow regimes. In the transitional flow regime the onset of transition occurred at a Reynolds number of 1 989. This also compared very well with a large body of literature. The general trend of results in the transitional flow regime also compared well to that of two previous experimental studies. However, exact comparisons were not possible as the boundary values of the different studies were not the same.

Furthermore, it can also be concluded that the validation results proved that the experimental set-up that was designed and constructed, the data reduction methodology, and experimental procedure that was implemented, produced accurate friction factor results. In addition the friction factor measurements can be produced in all three flow regimes of laminar, transitional and turbulent flow. This provided confidence that the original results produced in the following chapter, will be accurate.

4.3. Conclusion

The experimental setup and procedure, as well as the data reduction and results were validated in this chapter. The pressure drop was measured only across the fully developed region of flow for adiabatic conditions. The fully developed, adiabatic friction factors were then compared to literature. In the laminar, transitional and turbulent flow regimes it was found that the results compared well to literature. The onset of transition also compared favourably, commencing 4% earlier than previously predicted in literature, and was found to occur at a Reynolds number of 1 989. After the onset of transition the general trend of the transition curve also corresponded well with other studies.

5. Results: Adiabatic Pressure Drop

5.1. Introduction

This chapter is the most important of this study as its purpose is to present the results that were obtained experimentally. It is the logical outflow of the experimental set-up that was constructed in Chapter 3 and used to produce the results of this study. The validation experiments in Chapter 4 demonstrated that the results produced by the experimental set-up were accurate and provided reasonable proof that the results presented in this chapter are valid. This chapter produces the results aligned to the purpose of this study, which was formulated in Chapter 1 (to investigate the effect that presence of multiple tube entrances have on the adiabatic pressure drop in smooth and circular, horizontal tubes in the fully developed, transitional flow regime). Some of the results presented in this chapter are also compared to literature summarized in Chapter 2. Thereafter the results are critically discussed on different graphs, using a systematic approach by focusing on the laminar, turbulent and transitional flow regimes, respectively. The chapter ends with a summary, conclusions and recommendation for future work.

5.2. Scope and Summary of Experiments

For clarification, the purpose of this study and most critical parts of the experiments conducted are summarized in this section. All experiments were conducted on the same diameter and length of tube. Three smooth tubes with an inner diameter of 3.97 mm and length of 6 m were used as the test section. Pressure differential experiments were conducted in the length of the tube where hydrodynamic, fully developed flow occurred, and the pressure drops were measured between two pressured taps spaced 1.97 m apart. The pressure drops were measured with three pressure transducers coupled to three diaphragms with different accuracy and application ranges, to ensure that accurate pressure drops could be measured. All pressure differential measurements were conducted at different mass flow rates to ensure that results could be generated in the laminar, transitional, and turbulent flow regimes. From the pressure drop and mass flow measurements, the friction factors and Reynolds numbers were determined.

Two main sets of experiments were conducted. In Chapter 4, experiments were conducted on a single tube only, as validation experiments. A total of 53 friction factor measurements were collected at different Reynolds numbers. The results compared well with literature and provides a reasonable expectation that the second set of experiments (that address the purpose of this study) will be credible.

The second set of experiments discussed in the following section were conducted with the three tube test section. The three tubes of this test section were spaced a pitch distance of 8.4 mm or 1.4 outer diameters apart, measured from the centre line of each tube. A total of 69 experimental measurement points were presented, with 18 in the laminar flow regime, 21 in the transitional flow regime, and 20 in the turbulent flow regime. To simplify the presentation and discussion of the experiments, all the results of the second set of experiments are presented in Section 5.3 on one graph, together with the first set of experiments presented in Chapter 4, for comparative purposes.

5.3. Adiabatic Friction Factors

Figure 5.1 shows the adiabatic friction factors for each of the three tubes, for a range of Reynolds numbers from 700 to 5 100. The results are compared to the single tube results (Chapter 4), the Poiseuille [22] equation in the laminar flow region, and the Blasius [23] equation in the turbulent flow region. In the figure legend, the "Single Tube" refers to the test section consisting of a single tube, utilised in Chapter 4 for validation experiments and shown here for comparative purposes. "Tube 1", "Tube 2 (centre)", and "Tube 3" in the legend refer to the results from each of the three tubes in the three tube test section with "Tube 2" as the middle tube in the arrangement. The arrangement and number of the tubes is shown in the system schematic, Figure 3.1, and the schematic of the test section, Figure 3.3.

As many of the salient results are challenging to observe from Figure 5.1, the results are presented and discussed in separate subchapters, focusing first on the laminar flow regime (Section 5.3.1), secondly on the turbulent flow regime (Section 5.3.2), and then thirdly on the transitional flow regime (Section 5.3.3). The transitional flow regime is discussed last, as it is the original research contribution to this study. To simplify the discussion the mainly laminar flow results are discussed between Reynolds numbers of 700 and 1 780, transitional between 1 780 and 2 840, and turbulent between 2 840 and 5 100. It is emphasised that the ranges selected are not suggested as the transition points between different flow regimes, but were selected in this way to simplify the presentation and discussion of results.

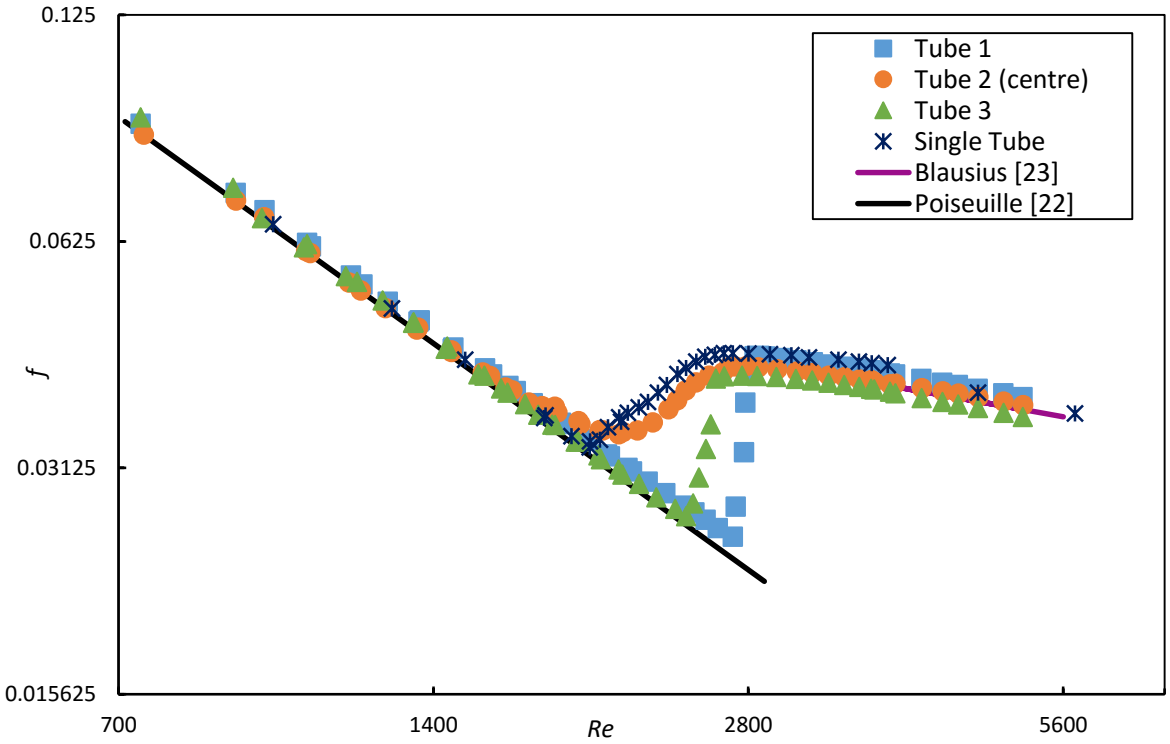

Figure 5.1: Adiabatic friction factors of the three tube test section compared to the single tube test section (Single Tube) as function of Reynolds number, illustrating the effect that three adjacent tube entrances have on transitional flow. The centre tube (Tube 2) is the tube spaced in the middle between Tube's 1 and 3. The Blasius and Poiseuille equations are also shown.

5.3.1. Laminar Friction Factors

The mainly laminar flow results are presented in Figure 5.2. The adiabatic friction factor results are for the single tube experiments as well as for the three tube experiments. The friction factor decreased for an increase in Reynolds number. In the data reduction, Equation 3.7.4 shows that friction factor is inversely proportional to the flow velocity, the pressure drop increases for an increase in flow rate, but the friction factor is proportional to the pressure drop over the square of the velocity. Therefore, the decreasing tend of the friction factor remains dominant in laminar flow.

The results are compared to the Poiseuille equation (2.2.2), prescribing that the friction factor for a smooth circular tubes is $f = 64/Re$. All the results compared well with both the Poiseuille equation and each other. The average error of the experiments compared to the Poiseuille equation was 2.4% and the maximum error was 6.5%, and occurred in Tube 1 at the point just before the start of the transitional regime. The adiabatic pressure drop, and thus the friction factor, was higher in the outer tubes than the middle tube, for Reynolds number less than 1 400. Tube 3 had a higher friction factor than Tube 1 for Reynolds numbers below 1 000. After this point Tube 3 had a lower friction factor than Tube 1.

The average error of the experiments (2.4%) was higher than the maximum uncertainty of the friction factors, which was less than 1%. It is challenging to identify the reasons that all the results were not within the uncertainty of the friction factors in the laminar flow regime. However, possible reasons were most probably combinations of the following: minor differences in the tube geometries (lengths and inner diameters), mixer geometries, flow meters, spacing between pressure taps, and installation of pressure tap holes.

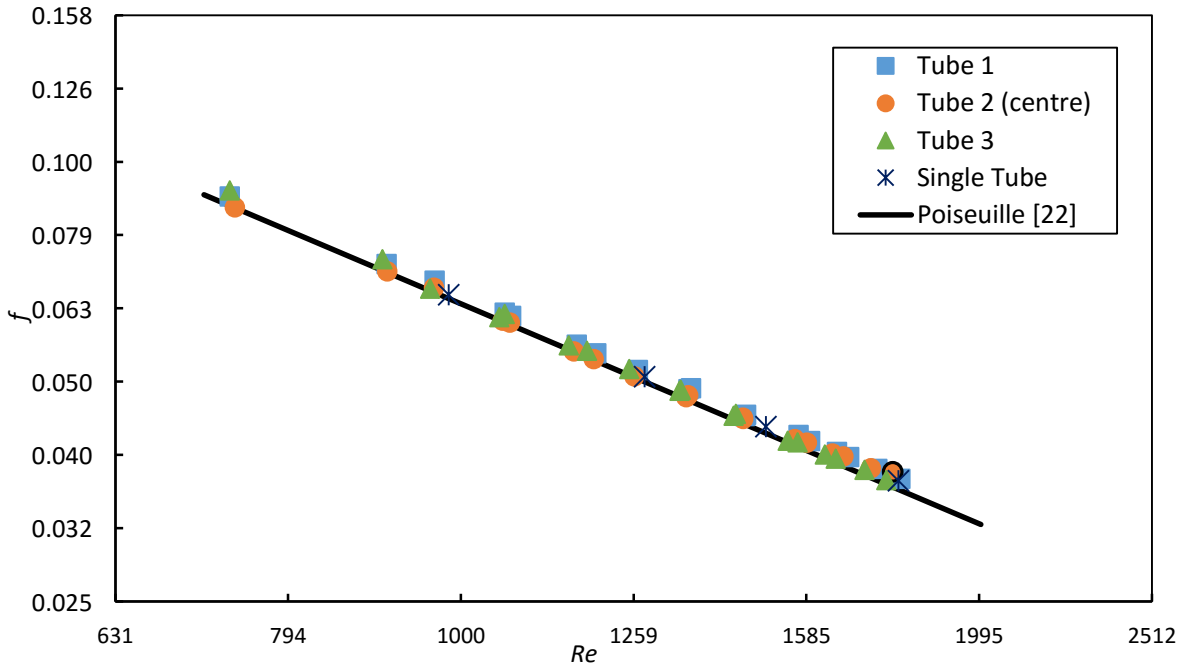

Figure 5.2: Adiabatic friction factors, in the laminar flow regime, of the three tube test section, as function of Reynolds number, illustrating the effect that three adjacent tube entrances have on laminar flow. The Single tube results and Poiseuille equations are also shown for comparative purposes. Re_{cr} is shown for Tube 2 with a marker outlined in black.

5.3.2. Turbulent Friction Factors

The experimental results of adiabatic friction factors as function of Reynolds number, in the primarily turbulent flow regime, are presented in Figure 5.3. The results are compared to the Blasius [23] equation (Equation 2.3.2), and to the validation results of the single tube experiments. In fully turbulent flow the friction factor resumed its decreasing trend for increasing flow rates and pressure drops. This was the same trend as seen in fully laminar flow (Equation 3.7.4).

The turbulent pressure drop across the centre tube held the closest relationship to the Blasius line, with a 1.3% average error between them. The pressure drop across Tube 1 was 3.1% higher, and the pressure drop across Tube 3, 3.1% lower, than that predicted by Blasius in the turbulent flow regime. The Blasius equation is valid for flow of Reynolds numbers greater than 4 000. However, from the results it was shown that results corresponded very well to the Blasius correlation at a lower Reynolds number. This point is referred to as Re_{FT}, in Figure 5.3, and indicates that the results showed full turbulent characteristics already at a Reynolds number of 3 220. This is not unusual as literature [11, 21] indicated that this might happen between Reynolds numbers of 3 500 and 10 000.

Fully turbulent flow is here defined as the flow for which the Blasius correlation is valid. The validity of the Blasius equation is stipulated as the point after which the percentage error, between each recorded friction factor data point and the Blasius line, is less than or equal to the average percentage error of the friction factors in each tube.

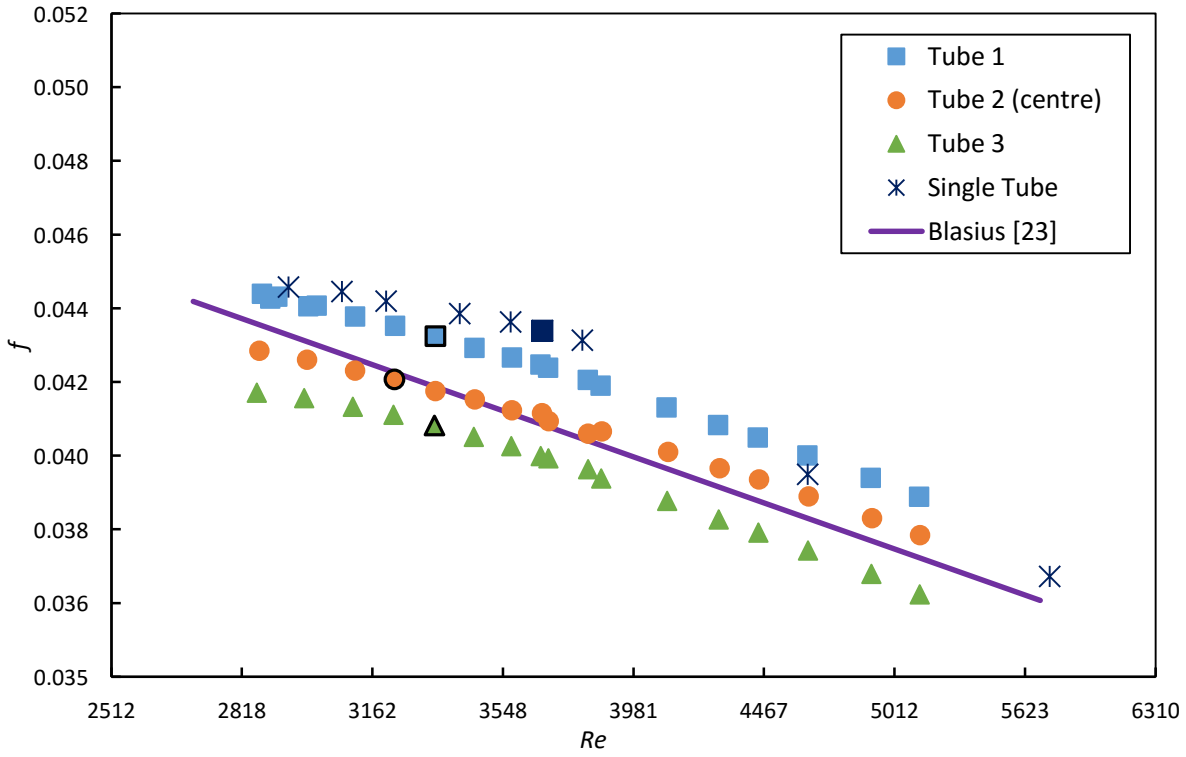

Figure 5.3: Adiabatic friction factors, in the turbulent flow regime, of the three tube test section, as function of Reynolds number, illustrating the effect that three adjacent tube entrances have on turbulent flow. The Single tube results and Blasius equations are also shown for comparative purposes. Re_{FT} points are shown outlined in black and as a solid marker for the single tube.

Table 5.1 summarises the Re_{FT} values for each of the tubes. Due to the symmetry of the tubes and the fact that turbulent flow is not influenced by inlet effects [9], the Re_{FT} point occurred at the same Reynolds number for the outer tubes. Fully turbulent flow was reached quicker for the centre tube (Tube 2), when compared to Tube 1 and Tube 3 and all three rubes in the three tube test section had lower Re_{FT} than that of the single tube in the validation experiments. This is due to the increased disturbance in the flow, experienced by the three tubes, which caused the onset of fully turbulent flow to occur sooner, with a maximum difference in the Reynolds numbers of 394 between the two experiments.

Table 5.1: Reynolds number where fully turbulent flow begins (Re_{FT}), and the Blasius equation becomes valid.

Tube	Re_{FT}
1	3 340
2 (Centre)	3 220
3	3 340
Single	3 614

For the outer tubes, the percentage error of the friction factor results, even in the fully turbulent regime, is higher than the 1% uncertainty error of the friction factor. Again, it is challenging to identify the reason, but it is most probably the same reasons listed for the laminar flow regime.

5.3.3. Transitional Friction Factors

The adiabatic friction factor data was plotted in Figure 5.4, and was compared to the single tube data and the Poiseuille equation. The boundary points of transition, where transition started, Re_{cr} and ended, Re_e, for all the tubes are summarised in Table 5.2. The points where transition started were identified as 2 724, 1 779 and 2 480 for tubes 1, 2 and 3 respectively. Similarly, the points where transition ended were identified as 2 839, 2 789 and 2 763.

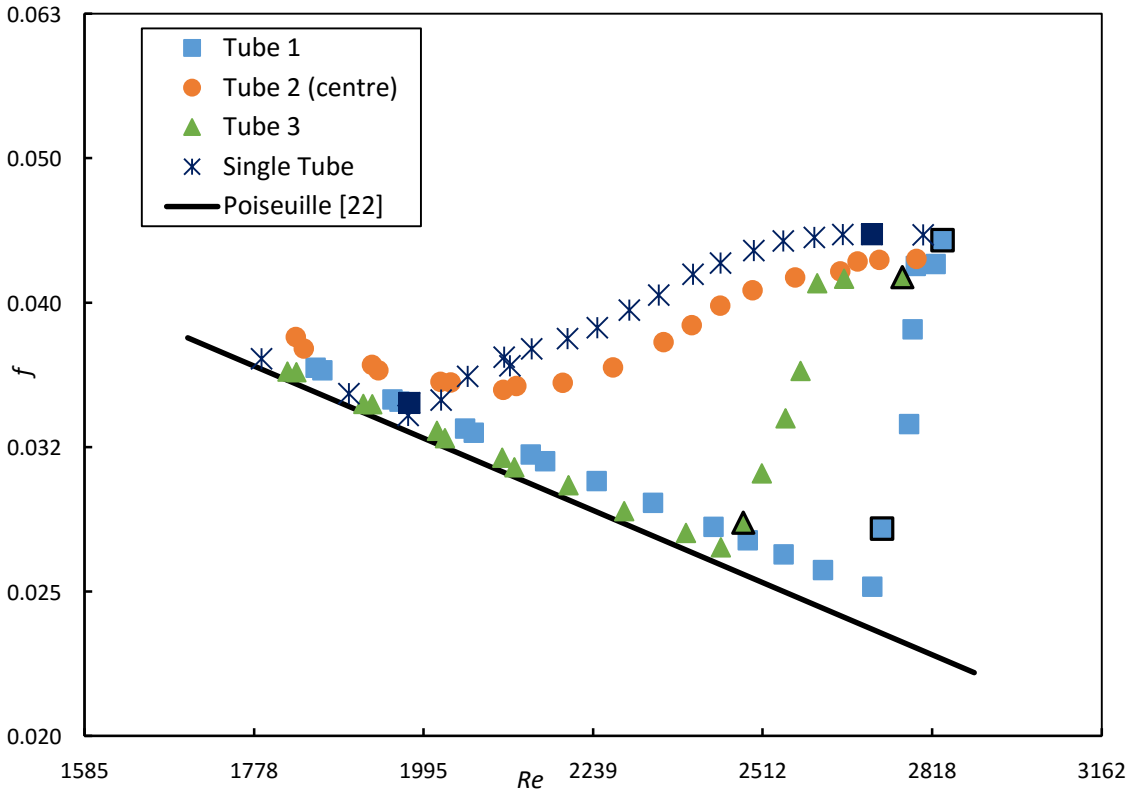

Figure 5.4: Adiabatic friction factors, in the transitional flow regime, of the three tube test section, as function of Reynolds number, illustrating the effect that three adjacent tube entrances have on transitional flow. The Single tube results and Poiseuille equations are also shown for comparative purposes. Re_{cr} and Re_e are shown as with markers outlined in black, and as solid markers for the single tube data.

Table 5.2: A comparison of the Reynolds numbers at which transition starts Re_{cr} and ends, Re_e, for each of the tubes in the three tube setup, as well as the single tube.

	Transition starts Re_{cr}	**Transition ends Re_e**	**Transition band Re_{cr}-Re_e**
Tube 1	2 724	2 839	115
Tube 2 (Centre)	1 779	2 789	1 010
Tube 3	2 480	2 763	283
Single	1 989	2 726	737

The centre (Tube 2) of the three-tube setup experienced an early commencement to transition at a Reynolds number of 1 779. This was earlier than the start of the single tube transition, which began at a Reynolds number of 1 989. This was likely to have occurred because of the disturbances introduced into the flow at the inlet, due the adjacent inlets. Tube 2 also experienced a transition with a bigger band (difference between Re_{cr} and Re_e) than that previously seen for a single tube. The centre tube also experienced a later end, Re_e, to the transitional flow regime than that seen for the single tube case, and the slope of the friction factor graph, in transition, was much gentler.

After a Reynolds number of 1 000, Tube 3, the friction factor in Tube 3 (Figure 5.2) was lower than that of Tube 1. However this altered again, as the onset of transition in Tube 3 occurred earlier than that of Tube 1.

At the end of the transitional flow regime, Tube 3 then returned to having a friction factor lower than Tube 1. The bandwidth of the transitional flow regime in the outer tubes (Tubes 1 and 3) was very narrow, with the start of transition being much delayed in both of the tubes and occurring at Reynolds numbers of 2 724 and 2 480, respectively. Consequentially, the gradient of the slope in transition was very steep.

The following correlation can be used to describe the adiabatic friction factor, in terms of Reynolds number, for transitional flow in tubes with three adjacent entrances. A correlation for the single tube case is also included. Table 5.3 summaries the coefficients of each of the correlations. The value in the last column of the table, R^2, is a measure of the goodness of fit of the trend line to the data. An R^2 value of 1 is a perfect fit, therefore all of the equations correlate well to the measured data. The equation for Tube 1 had the lowest goodness of fit value, of 0.88 which can still be concluded as a reasonable fit.

$$f = a + bRe + cRe^2 + dRe^3 \tag{5.2.1}$$

Table 5.3: Curve-fit equations' coefficients for adiabatic friction factor in the transitional flow regime, as a function of Reynolds number, for each of the tubes.

	a	b	c	d	R^2
Tube 1	-6.37	$4.47\text{x}10^{-3}$	$-7.78\text{x}10^{-7}$	0	$8.75\text{x}10^{-1}$
Tube 2 (Centre)	$5.33\text{x}10^{-1}$	$-6.45\text{x}10^{-4}$	$2.73\text{x}10^{-7}$	$-3.76\text{x}10^{-11}$	$9.82\text{x}10^{-1}$
Tube 3	-1.89	$1.42\text{x}10^{-3}$	$-2.61\text{x}10^{-7}$	0	$9.45\text{x}10^{-1}$
Single	$5.01\text{x}10^{-2}$	$6.14\ \text{x}10^{-5}$	$-9.7\text{x}10^{-9}$	0	$9.88\text{x}10^{-1}$

In the three tube setup up, the results showed that the centre tube (Tube 2) experienced a different transition to the Single tube case, due to the increased disturbance caused by the adjacent tubes at the inlet. These adjacent tubes also experienced a different transition to the Single tube, with the start of tradition being delayed. It appeared that the presence of the centre tube caused a smoothing effect on the inlet of the adjacent tubes, delaying the start of the transitional flow regime. With all three tubes experiencing transitional flow this smoothing effect ceased and caused the pressure drop across the outer tubes to increase abruptly before the flow became turbulent. The differences between the two outside tubes (Tube 1 and Tube 3) are discussed in Section 5.4.

5.4. Symmetry and Maldistribution of Flow

Due to the symmetry about the centre tube in the geometry of the three tube test setup, it could reasonably be expected that the results for Tube1 and Tube 3 be identical. However, it is clear from Figures 5.1 and 5.4, that the adiabatic friction factor in the transitional and turbulent flow regimes is different for the two outer tubes.

Figure 5.5 illustrates the difference in the mass flow rates of each tube as the flow rate was increased throughout the testing procedure. The horizontal axis denotes the duration of the test as the mass flow rate was increased and is represented by the number of the data point taken at each flow rate. Logically, data point one was the first measurement taken at the lowest mass flow rate of 0.0028 kg/s and data point 33 was the last, at 0.013 kg/s.

The two black vertical lines show the start and end of the transitional flow regime, with transition ending at the same data point (but not Reynolds number) for all three tubes. The dotted black line shows the start of the transitional flow regime in the centre tube while the solid black line shows the start for the adjacent tubes.

In the first part of the laminar flow regime, the flow rates of tube one and three were almost identical, with a 0.5% difference between the two tubes. Upon the start of the transitional flow regime in the centre tube, tube one started to experience a higher flow rate than tube 3. Once tube one and three experienced transition, the difference in mass flow rates increased until there was a 5.8% difference between them. In turbulent flow this drops down to a 0.1% difference in flow rates. This difference may be partly due to the inherent uncertainty of the mass flow meters. The flow rates in all the tubes were adjusted each day to within 0.05 l/hr of each other by controlling the clamps on the downstream hose.

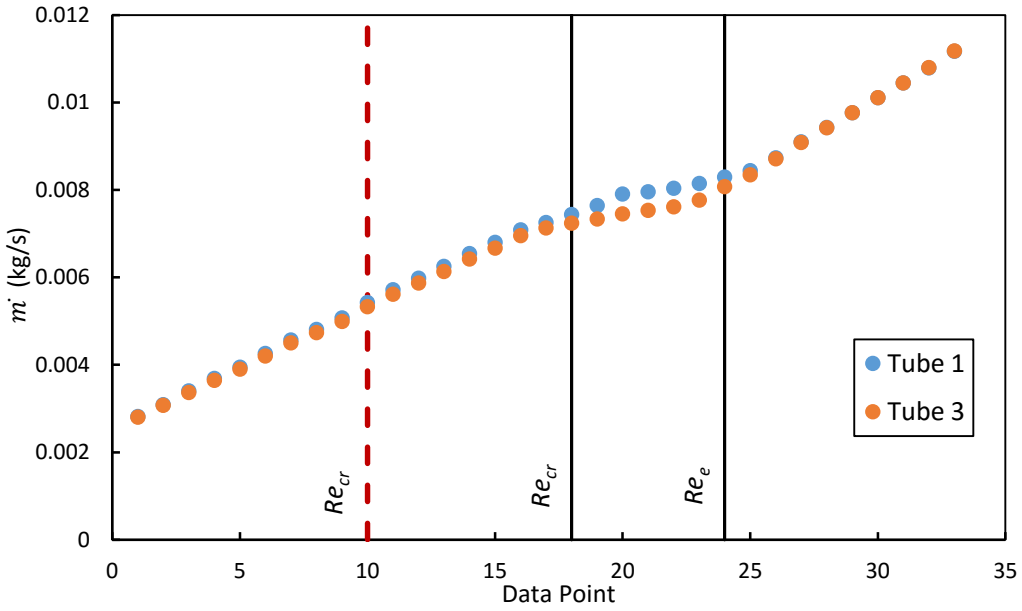

Figure 5.5: The mass flow rate in the adjacent tubes for each data point that was collected, starting in laminar flow and increasing the mass flow rate into the turbulent flow regime. The solid black lines indicate the start, Re_{cr}, and end, Re_e, of transition in the adjacent tubes (Tubes 1 and 3). The dotted red line shows the start of transition in the centre tube.

Laminar tube flow has the characteristic of being able to 'detect' downstream effects. This means that if the resistance in any one of the tubes was slightly different, that would cause a difference in the flow rates. Clamping the downstream hoses was undertaken in an attempt to neutralise this effect, and therefore only the inlet effects should have disturbed the flow. Utilising the hose clamps to equalise the flow was a relatively crude method of creating the same tube resistance. Using valves or iterating the plant build until the system resistances are equal in each tube is a more accurate method to measure the flow maldistributions. However, assuming that the tube resistances are made approximately equal by the clamps, the difference seen in the flow rates was then due to the inlet effects. This explains the difference between the friction factors in Tube 1 and 3 in the laminar flow regime, as shown in Figure 5.2.

With the start of transitional flow in the centre tube, the outer tubes also experienced a flow maldistribution, with Tube 1 one experiencing a higher mass flow rate than Tube 3. This phenomenon was observed over several days of testing and was therefore an inherent characteristic of the inlet of the test setup.

In Figure 5.3 the friction factors of Tube 1 and Tube 3 differed 5.6% in the fully turbulent flow regime, and yet the flow rates were approximately the same, as shown in Figure 5.5. Therefore in the turbulent flow regime there occurred a maldistribution, not of the mass flow rate, but of the pressure drop in the tubes. This is illustrated in Figure 5.6 where the pressure drop of both the outer tubes is plotted against Reynolds number. The tubes experienced an equal pressure drop in the laminar flow regime. With the onset of transitional flow, the pressure drops across the tubes increased as expected. Tube 3 experienced this sudden increase first, as was already shown in Figure 5.4 of the friction factors. At the termination of transition, Tube 1 had a higher pressure drop than Tube 3. This trend continued into fully turbulent flow with a difference in pressure drop between the two tubes of 5.4%.

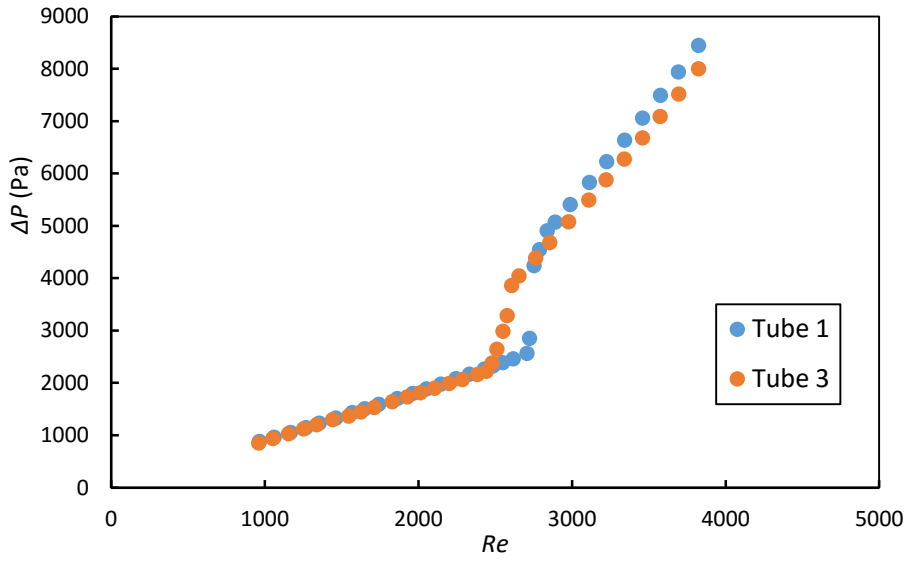

Figure 5.6: Adiabatic pressure drop as a function of Reynolds number, for the outer tubes in the three tube test section.

5.5. Conclusions

The aim of this chapter was to investigate the adiabatic friction factors experienced by each of the tubes in the three tube setup, as well as to compare them to the results found for the single tube test. In the laminar flow regime, all three tubes followed the trend expected from previous work. There were small differences in the friction factors for each tube. However, this was shown to be due to the flow maldistribution caused by the inlet disturbances when the flow in the centre tube became transitional. It was found that the centre tube experienced an earlier onset of transitional flow than the single tube and that the start of the transitional flow regime in the outer tubes was much delayed. The effect of having multiple, adjacent inlets caused a maldistribution in the flow, and thus a 5.8% difference in the flow rates of the outer tubes. The end of the transitional flow regime occurred in a relatively small band for all three tubes. Curve-fit equations were fashioned for each of the tubes, in order to calculate the adiabatic friction factor as a function of Reynolds number.

The friction factor of all three tubes, in the turbulent flow regime, followed the trend predicted by literature. After the end of the transitional flow regime, all three tubes reached a state of fully turbulent flow in a relatively small margin, with the centre tube being somewhat more rapid in this change due to its smooth transition from laminar to turbulent flow. In the turbulent flow regime the mass flow rate was uninfluenced by the inlet or downstream effects, however, a maldistribution of the pressure drop occurred, with Tube 1 having a higher pressure drop than Tube 3 across its length, in this flow region.

For future studies it would be useful to control the flow in each tube by inserting flow control valves. Also, by managing the resistance of each tube so that they are all the same, these maldistribution effects could be better understood.

6. Summary, Conclusion and Recommendations

6.1. Summary

Heat exchangers have many applications in a variety of industries such as aerospace, heating, ventilation, and cooling, as well in energy generation industries such as nuclear, concentrated solar power, and fossil fuel power. Shell-and-tube heat exchangers are one of the most common form of heat exchanger used and they are traditionally designed to operate in the turbulent flow regime, in order to make use of the higher heat transfer that this regime offers. However, the higher pressure drops experienced in turbulent flow make the design and build of these heat exchangers expensive, and the operation of them more risky. Design in the transitional flow regime is therefore, being increasingly considered. Manufacturers in regions of the world with very low winter temperatures are designing heat exchangers with glycol mixtures as the working fluid. The high fluid viscosities tend to force the operating mass flow rates to fall close or into the transitional flow regime. It is also necessary to understand transitional flow in already operating heat exchangers, where deposit build-up has caused the mass flow rate to decrease into the transitional flow regime.

Fluid flow in tubes has been under investigation since 1883. Laminar and turbulent flow and their pressure drop characteristics are well understood. Only more recently has the transitional flow regime been investigated. However, the work so far has been limited to single, smooth tubes with different inlet geometries, for developing and fully developed flow. There has also been some research into nanofluid flow in transition as well as transitional flow in micro-tubes. However, there exists a research gap where the effect of multiple tube entrances is quantified in terms of pressure drop in the transitional flow regime. Therefore, the purpose of this study was to experimentally investigate the effect of multiple tube entrances on the pressure drops in the transitional flow regime.

Two test setups were built for this study: a single tube setup, used for validation purposes and a three tube setup, to test the effect that multiple inlets have on the adiabatic pressure drop in the transitional flow regime. The tubes used in both of these setups were 6 m long stainless steel tubes with an inner diameter of 3.97 mm. Both the single tube and the three tube setup were alternatively attached at the inlet to a calming section with a square-edged inlet shape. Water was used as the working fluid. The inlet and outlet temperatures were measured using PT100 probes. The pressure drop was measured in the fully developed section of flow in the last 1.97 m of the tube, between two pressure taps. A variety of carefully selected diaphragms were used to measure the pressure differential. The entire test section between the temperature measuring probes was insulated to ensure that were was no heat transfer to and from the environment. The entire experimental bench was situated in an enclosed laboratory which was maintained by air-conditioning at 23^{o}C.

An uncertainty analysis was performed based on the technical specification of the instrumentation used, calibrated data and all of the data collected. The Reynolds number was found to have an uncertainty of less than 2%, while the friction factor uncertainty was less than 1%. The experimental test bench, the test setup and the data reduction method was validated by testing the single tube setup and comparing it to literature. Comparisons were made in the laminar, transitional, and turbulent flow regimes. The results compared well with literature.

6.2. Conclusions

Experiments were conducted on the single tube test section for a range of 750 to 9 300 Reynolds number. The comparison to literature was satisfactory, with a 1.5% error in the laminar, and 2% error in the turbulent flow regimes. The friction factor curve had the same shape in the transitional flow regime as that seen in literature, with the start of transition occurring 4% earlier. It was concluded that this was due to the size tube, the difference in working fluid and the fact that pressure drop was measure only in fully developed flow for this study. Therefore, the single tube tests successfully validated the experimental setup.

The three tube setup was tested, with 69 data points of adiabatic friction factor collected in the Reynolds number range of 700 to 5 100. In the laminar flow regime, there were small differences in the friction factors for each tube. The average error of the experiments, compared to theory, was 2.4%. This was higher than the maximum uncertainty of the friction factors. Possible reasons for this occurrence were most probably combinations of the following: minor differences in the tube geometries (lengths and inner diameters), mixer geometries, flow meters, spacing between pressure taps, and installation of pressure tap holes.

It was found that the centre tube experienced an earlier onset of transition than previously seen for the single tube and that the start of the transitional flow regime in the outer tubes was much delayed. The effect of having multiple, adjacent inlets caused a maldistribution in the flow, and thus a 5.8% difference in the flow rates of the outer tubes. The end of the transitional flow regime occurred in a relatively small band for all three tubes. Curve-fit equations were fashioned for each of the tubes, in order to calculate the adiabatic friction factor as a function of Reynolds number.

The friction factor of all three tubes, in the turbulent flow regime, followed the trend predicted by literature. After the completion of the transitional flow regime, the three tubes all reached a state of fully turbulent flow in a relatively small margin, with the centre tube being somewhat sooner because of its smooth transition from laminar to turbulent flow. In the turbulent flow regime the mass flow rate was uninfluenced by the inlet or downstream effects. However, the pressure differential of each tube, when compared, was uneven, with Tube 1 seeing the highest pressure drop.

In general, it can be concluded that the inlets of multiple tubes adjacent to each other have a significant influence on the pressure drop across the fully developed length of each tube, specifically in the transitional flow regime.

6.3. Recommendations

Following the results of this study, it is recommended that the subsequent subjects be investigated:

- Compare the pressure drop in three tubes with different inlet pitch distances. In this study only one pitch was studied due to time and funding constraints. However, investigating the most efficient pitch distant will improve shell-and-tube heat exchanger design.
- Inlet effects of multiple tube entrances in two planes. Therefore, have an arrangement of four in-line tubes or five staggered tubes and study the effect on pressure drop in the laminar, transitional and turbulent flow regimes.

- Flow and pressure maldistributions for multiple tube entrances could be better understood by managing the resistance of each tube so that they are all functionally identical.
- Investigate only inlet effects more accurately by precisely controlling the flow in each tube with valves.

References

[1] H. Lund, Renewable energy strategies for sustainable development, Energy, 32(6) (2007) 912-919.

[2] J.P. Meyer, Heat Transfer in Tubes in the Transitional Flow Regime, Proceedings of the 15th International Heat Transfer Conference, Kyoto, Japan, 2014.

[3] K. Craig, J.P. Meyer, W.G. Le Roux, Computational fluid dynamics analysis of parabolic dish tubular cavity receiver, Proceedings of the 3rd Southern African Solar Energy Conference, South Africa, 11-13 May, 2015., 2015.

[4] R. Shah, D. Sekulic, Handbook of Heat Transfer: Heat exchangers, Wiley, New York, 1998.

[5] L.-M. Tam, A.J. Ghajar, Effect of inlet geometry and heating on the fully developed friction factor in the transition region of a horizontal tube, Experimental Thermal and Fluid Science, 15(1) (1997) 52-64.

[6] A.J. Ghajar, L.-M. Tam, Heat transfer measurements and correlations in the transition region for a circular tube with three different inlet configurations, Experimental Thermal and Fluid Science, 8(1) (1994) 79-90.

[7] A.J. Ghajar, K.F. Madon, Pressure drop measurements in the transition region for a circular tube with three different inlet configurations, Experimental Thermal and Fluid Science, 5(1) (1992) 129-135.

[8] H.K. Tam, L.M. Tam, A.J. Ghajar, Effect of inlet geometries and heating on the entrance and fully-developed friction factors in the laminar and transition regions of a horizontal tube, Experimental Thermal and Fluid Science, 44(0) (2012) 680-696.

[9] J.A. Olivier, J.P. Meyer, Single-phase heat transfer and pressure drop of the cooling of water inside smooth tubes for transitional flow with different inlet geometries (RP-1280), HVAC and R Research, 16(4) (2010) 471-496.

[10] J.A. Olivier, J.P. Meyer, Single-Phase Heat Transfer and Pressure Drop of the Cooling of Water inside Smooth Tubes for Transitional Flow with Different Inlet Geometries, HVAC&R Research, 16(4) (2010).

[11] J.P. Meyer, J.A. Olivier, Transitional flow inside enhanced tubes for fully developed and developing flow with different types of inlet disturbances: Part I - Adiabatic pressure drops, International Journal of Heat and Mass Transfer, 54(7-8) (2011) 1587-1597.

[12] J.P. Meyer, J.A. Olivier, Transitional flow inside enhanced tubes for fully developed and developing flow with different types of inlet disturbances: Part II-heat transfer, International Journal of Heat and Mass Transfer, 54(7-8) (2011) 1598-1607.

[13] W. Nunner, F. Hudswell, Heat transfer and pressure drop in rough tubes, Atomic Energy Research Establishment, 1958.

[14] J.P. Meyer, T. McKrell, K. Grote, The influence of multi-walled carbon nanotubes on single-phase heat transfer and pressure drop characteristics in the transitional flow regime of smooth tubes, International Journal of Heat and Mass Transfer, 58(1) (2013) 597-609.

[15] J. Dirker, J.P. Meyer, D.V. Garach, Inlet flow effects in micro-channels in the laminar and transitional regimes on single-phase heat transfer coefficients and friction factors, International Journal of Heat and Mass Transfer, 77 (2014) 612–626.

[16] M. Everts, Heat Transfer and Pressure Drop of Developing Flow in Smooth Tubes in the Transitional Flow Regime, University of Pretoria, 2014.

[17] K. Wang, X.C. Tu, C.H. Bae, H.B. Kim, Optimal design of porous baffle to improve the flow distribution in the tube-side inlet of a shell and tube heat exchanger, International Journal of Heat and Mass Transfer, 80 (2015) 865-872.

[18] TEMA, Standards of the Tubular Exchanger Manufacturers Association, in: Mechanical Standards TEMA Class R C B, Standards of the Tubular Exchanger Manufacturers Association Inc., New York, 1999, pp. 29.

[19] O. Reynolds, An experimental investigation of the circumstances which determine whether the motion of water shall be direct or sinuous, and of the law of resistance in parallel channels, Proceedings of the royal society of London, 35(224-226) (1883) 84-99.
[20] F.M. White, Fluid mechanics, WCB, McGraw-Hill, Boston, 1999.
[21] Y.A. Çengel, A.J. Ghajar, Heat and mass transfer: fundamentals & applications, McGraw-Hill, New York, 2011.
[22] J.L. Poiseuille, Recherches expérimentales sur le mouvement des liquides dans les tubes de très-petits diamètres, Imprimerie Royale, 1844.
[23] H. Blasius, Das Ähnlichkeitsgesetz bei Reibungsvorgängen in Flüssigkeiten, Springer, 1913.
[24] X. Fang, Y. Xu, Z. Zhou, New correlations of single-phase friction factor for turbulent pipe flow and evaluation of existing single-phase friction factor correlations, Nuclear Engineering and Design, 241(3) (2011) 897-902.
[25] K. Mohammadi, M.R. Malayeri, Parametric study of gross flow maldistribution in a single-pass shell and tube heat exchanger in turbulent regime, International Journal of Heat and Fluid Flow, 44(0) (2013) 14-27.
[26] J.C. Gibbings, Diffusion of the intermittency across the boundary layer in transition, Proceedings of the Institution of Mechanical Engineers, Part C: Journal of Mechanical Engineering Science, 217(12) (2003) 1339-1344.
[27] B.S. Petukhov, A.F. Polyakov, B.K. Strigin, Heat Transfer in Tubes With Viscous-Gravity Flow, Heat Transfer-Soviet Research, 1(1) (1969) 24-31.
[28] A.J. Ghajar, C.C. Tang, W.L. Cook, Experimental investigation of friction factor in the transition region for water flow in minitubes and microtubes, Heat Transfer Engineering, 31(8) (2010) 646-657.
[29] R. Rayle, Influence of orifice geometry on static pressure measurements, in, American Society of Mechanical Engineers, 1959.
[30] A. Bakker, R.D. LaRoche, E.M. Marshall, Laminar flow in static mixers with helical elements, in: The online CFM Book, http://www. bakker. org/cfm, 1998.
[31] C.O. Popiel, J. Wojtkowiak, Simple Formulas for Thermophysical Properties of Liquid Water for Heat Transfer Calculations (from 0°C to 150°C), Heat Transfer Engineering, 19(3) (1998) 87-101.
[32] P.F. Dunn, Measuring and Data Analysis for Engineering and Science, 2nd ed., CRC Press, Boca Raton, 2010.